A New Approach to Designing the Conical Point of a Twist Drill

Minhui Li

A Thesis

In the Department

Of

Mechanical and Industrial Engineering

Presented in Partial Fulfillment of the Requirements

For the Degree of Master of Applied Science at

Concordia University

November 2016

CONCORDIA UNIVERSITY

School of Graduate Studies

This is to certify that the thesis prepared

By: ___Minhui Li_____

Entitled: ___A New Approach to Designing the Conical Point of a Twist drill___

and submitted in partial fulfillment of the requirements for the degree of

___Master of Applied Science (Mechanical Engineering)_____

complies with the regulations of the University and meets the accepted standards with respect to

originality and quality.

Signed by the final examining committee:

_____Dr. Brandon Gordon_____ Chair

_____Dr. Sivakumar Narayanswamy_____Examiner

_____Dr. Zhenhua Zhu_____ Examiner

_____Dr. Chevy Chen_____ Supervisor

Approved by _____

Chair of Department or Graduate Program Director

_____

Dean of Faculty

Date _____

Abstract

A New Approach to Designing the Conical Point of a Twist Drill

Minhui Li

The point geometry of a twist drill is the most significant part which may affect to cutting performance in the drilling process. However, it is really complicated to establish an exact mathematic equation to represent the conical flank surface of a twist drill. In order to simplify problem and meet the practical engineering demand in the industry, this research focuses on developing an approximate mathematic model of the conical drill point geometry.

Additionally, an integrated CAD/CAM software is developed. This software integrates the modeling function of flute, margin, point and split features and is able to calculate grinding path of each feature. With the help of this software, drill geometric parameters can be modified reasonably according to different requirements easier than ever.

Finally, this research also mentions a CAD/CAM/CAE application to evaluate the cutting performance of a twist drill. The designed 3D model can be imported in *Thridwave* to predict cutting force, torque and peak temperature during the drilling process. Based on these simulative factors, the cutting performance of a twist drill can be generally evaluated. Four evaluated designs were selected and ground by 5-axis CNC grinding machine. The geometry of the ground drill shows a good agreement with the dimension of each design parameter, which validates the accuracy of the proposed modeling method and the corresponding grinding path.

Acknowledgements

I would first like to thank my supervisor, Dr. Chevy Chen, for his kind guidance and patient instructions through all this work. Dr. Chen's door was always open whenever I ran into a trouble or had a confusion to my research. I also need to appreciate Dr. Chen bringing me to Zhuzhou Cemented Carbide Cutting Tools Ltd. for a month internship, where I learned a lot of practical experience.

In addition, I would like to appreciate Tao Zeng who provided the idea which was a great help to my thesis. Especially, the content of Chapter 2 is under the guidance of Tao Zeng. Besides, I should thank you all my senior fellows, Mohsen Habibi, Chun Du, Liming Wang, Stephan Fong, Jiapu Zhu, Leo Chang for their kindly instructions. No matter when I asked questions from them, they would always stop what they were doing to hear me and help me out.

Finally, I also would like to thank my parents for their consistent support and all my friends for accompanying me all the way during my hard time.

List of Contents

List of Figures

List of Tables

Chapter 1.   Introduction

1.1. Basic of Conical Drill Point Design

1.1.1.   Twist drill point

The drill is the cutting tool most commonly associated with producing machined holes because it is simple, quick and economical. Approximately 25% of the metal cutting processes are drilling operations and approximately 40% of work-piece materials are removed by drills [1] Drilling is one of the most complex machining processes, because the drilling process combines the cutting operation in the circumferential direction and the extruding operation in the axial direction. Drilling process demonstration can be seen in Fig. 1.1. The high thrust force is produced by the feeding motion when the drill first extrudes metal under the chisel edge and then the cutting lip will shear the rest of the material. During this period, the cutting force and temperature start to rise up rapidly which may result in a serious wear on the cutting lip. These all happen on drill point. Therefore, the proper design of drill point can bring substantial savings in drilling costs and apparent rise for the drilling efficiency.

Drill point design is highly determined by the size of the drill and the material to be drilled. Today's material varies from an easy-to-drill material to the one that can be very troublesome. For some hard-to-drilling alloy steel, the drill must be made with less rake angle for providing enough rigidity in the tool and maximum support and strength to the cutting lip. However, less rake angle can accelerate wears to the cutting lip because of higher thrust value and excessive heat generation, which means lower efficiency and high machining cost. Therefore, the concept

1

of a successful drill point design should be able to increase the efficiency as much as possible

without weakening the cutting lip to the point for extending drills service life.
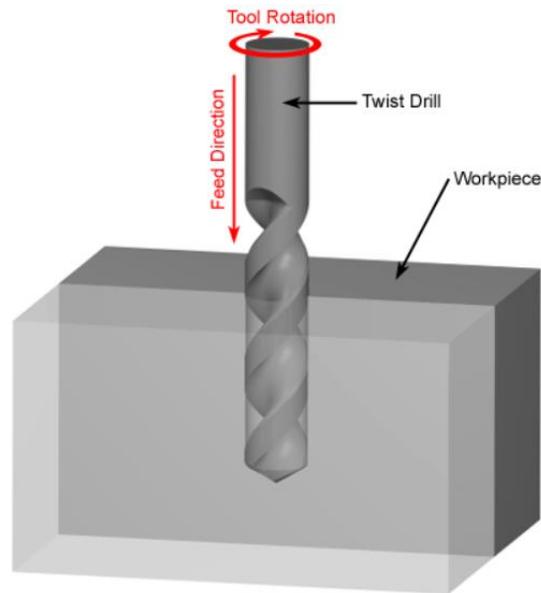
Figure 1.1 Drilling process

1.1.2. Design parameters of conical twist drill point

Design parameters determine the geometry and the structure of a drill. Once the material is

specified, the geometry of the drill point has a decisive influence on the cutting performance

which is able to directly affect the cost and efficiency of the manufacturing process. There are

three most significant design parameters, as shown in Fig 1.2, can determine the structure and

geometrical characteristic of a conical drill point: point angle, chisel edge angle, lip relief angle.

1) Point angle: The angle of 118° is used for a general purpose. For hardened and tough

   material, this value should be larger, in order to provide a sharper and stronger cutting

   lips.

2) Chisel edge angle: Chisel edge angle is used for describe chisel edge. Chisel edge is the intersection line of two conical flank surfaces located at the end of the drill point. It can be considered as a cutting lip with an extremely negative angle. When the drill point working onto the material, the way that chisel edge works is actually extruding hardly into the material instead of shearing the workpiece which may generate the enormous thrust force and the excessive heat. However, chisel edge cannot be completely removed, because it enables the drill to get a better self-centering ability while the drilling process.

3) Lip relief angle (lip clearance angle): This parameter is the relief angle measured at the outer point on the cutting lip. A certain amount of relief angle can avoid a great generation of heat caused by the friction between the flank surface and the workpiece, but too much of it can weaken the strength of the cutting lip.
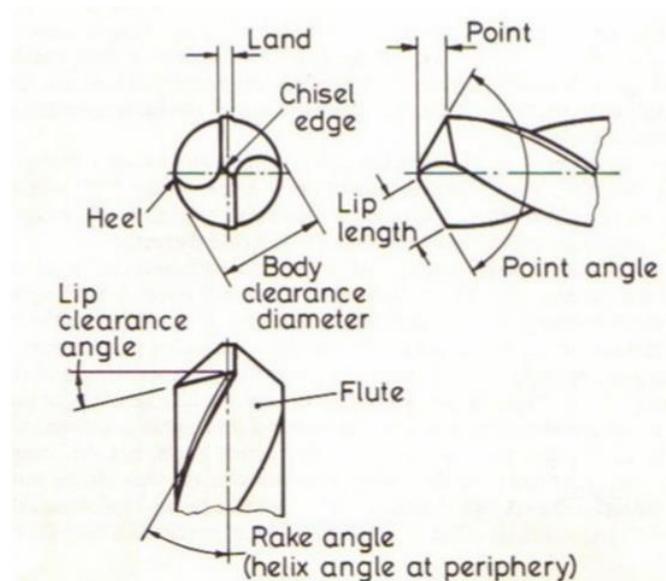
Figure 1.2 Nomenclature of conical twist drill point

1.1.3. Grinding parameters to conical drill point

The flank surface of conical drill point is grounded by a pair of cone surfaces. Previously, CNC grinding machine is not equipped in many workshops. Drill points are grounded by skilled mechanist or tool maker. This skill is highly unstable and relied on the practical experience. With the development of CNC technology, today's drill point can be precisely grounded by 5-axis grinding machine. By setting up the motion of a grinding wheel in five different degrees of freedom (three translational motions and two rotary motions), the grinding wheel can be positioned to the designated location and configured to grind along a particular grinding path. Grinding parameters are used for describing this motion in CNC machine and ensure the grinding wheel to grind a precise drill point.

1.2. Parametric Design

In parametric design, inter-related parameters of each geometric feature make up a predetermined constraint in geometry. Once the value of a dimension is slightly changed, the known entities would yield a completely different picture altogether. [1] It is well known that the conical twist drill point is formed by a constant motion of grinding wheel in accordance with a pair of conical surfaces, the place of which is determined by a group of grinding parameters. However, the reality is, in the normal design task, design parameters are the initially given condition. To guarantee that the drill point can be well-machined, a precise mathematic model which enables to convert grinding parameters from design parameters is required. In this research, based on the grinding parameters, it is available to derive the expression of the conical surface in terms of the drill coordinate system. The equation of the flank surface is the same as the generated conical surface. Design parameters, afterward, can be easily represented according

to the geometric structure of the conical flank surface. Consequently, the corresponding relationship between grinding parameters and design parameters can be built. This mathematic model and solution of grinding parameters will be discussed in details in Chapter 2.

1.3. CATIA Macro Programming with Visual Basic.Net

CATIA (Computer-Aided Three-dimensional Interactive Application), as one of the most powerful CAD system, is widely used in the geometric modeling work. [2] Macro offered in CATIA allows the user to automatically create complicated 3D geometric elements. It is possible to involve a series of functions written in a programming language and pack into a single command to perform a task repeatedly. This technique gives a good way to increase the efficiency and maximum reduce the possibility of human errors in repetitive tasks. Vb.net is a programming language, which can provide an independent and user-friendly interface running on Windows and it also can be used for macro programming. This research takes advantage of macro programming and develops an integrated CAD/CAM software to design a twist drill. With several easy steps, the 3D solid model of a twist drill can be automatically built in CATIA and the relative manufacturing information will be outputted as well. The application of this software is introduced in Chapter 3.

1.4. Problem and Objective of Thesis

Since the variety of materials to be drilled requires the great variety of drill type, it is important to modify drills geometry quickly, accurately. Therefore, the problems to be solved in this research are:

1) It is hard to establish an exact mathematic model to the drill point because the drill point is extremely complicated in geometry and also highly related to the shape of other features. A simplified flank surface mathematic model that can solve a practical problem in an efficient way is required.

2) Generating a 3D model involves tons of repetitive modeling operations. It demands the designer to reach a proficiency level of 3D modeling abilities as well as the knowledge of CNC machining. A software which can build accurate 3D model for previewing structure and output grinding path based on a particular machining tool is required.

3) Normally, the cutting performance of a newly designed drill point should be evaluated by numerous drilling experiments. In order to save the cost of the experiment, it is important to make use of FEA software to predict cutting force, torque and peak temperatures. Thus, a reliable way to predict the cutting performance is required.

In consideration of above practical problems, it is highly demanding to develop a comprehensive mathematic model to quickly generate the visible 3D model. An integrated automatic modeling software and an efficient prediction method are also needed. Thus, the objectives of this research are:

1) To derive a new approximate mathematic model for the twist drill point geometry in the form of conical flank surfaces to meet the practical engineering demands. This developed mathematic model can not only be established without relying on the flute feature, but also deduce the relationship between design parameters (semi-point angle, chisel edge angle, structural relief angle) and grinding parameters (a rotated angle and three

translated distances, semi-cone angle). The flowchart of the deduction process can be seen in Fig.1.3. It provides more freedom to the structure of the drill point design.
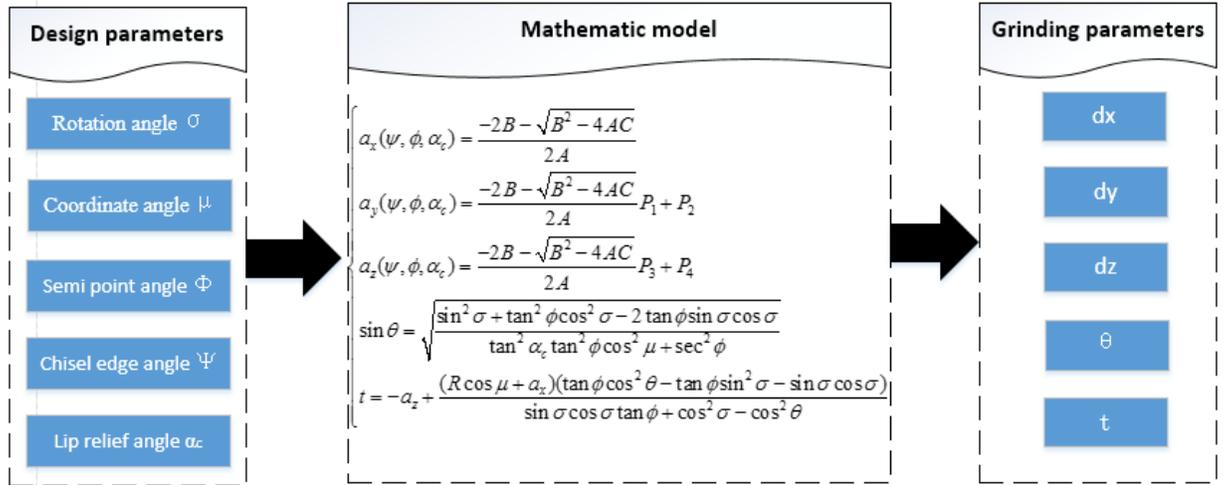
Figure 1.3 The deduction process of the mathematic model

2) In order to enhance the practicability, an integrated CAD/CAM twist drill modeling software is developed. This software is controlled by programming language vb.net and able to automatically generate 3D model in CATIA by making use of the established mathematic model. This software provides a clear and user-friendly interface, from where users can configure 5-axis machining tool and set up grinding wheels. The software also provides separate design workbenches for four features: flute, margin, point and split, as can be seen in Fig.1.4 . Users are allowed to change design parameters to modify the drill geometry in CATIA easily. The software will build all expected features step by step in CATIA and output grinding path after each modeling procedure until finishing an entire twist drill 3D model. The generated 3D model can be imported into analysis software to

evaluate drilling performance and the outputted grinding path can be converted into G-code as the manufacturing information to CNC machine.
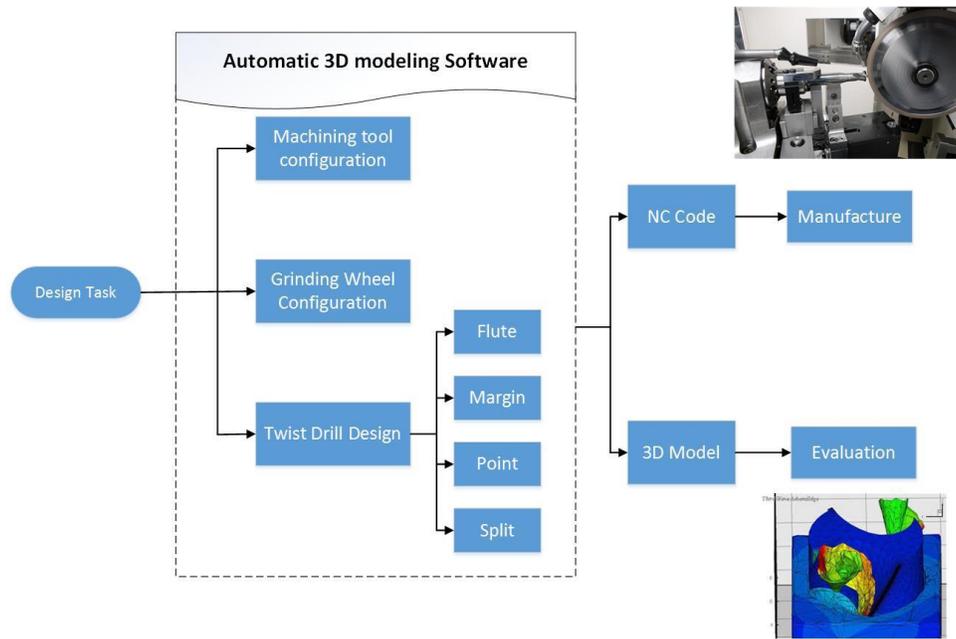
Figure 1.4 The use of the integrated CAD/CAM software in twist drill design

3) An integrated CAD/CAM/CAE method is used for predicting cutting performance of drilling process in a simulation software *Thirdwave.* In the simulation, thrust, torque and peak temperature during the drilling process can be predicted and estimate the cutting performance.

1.5. Literature Review

For the conical drill point, many researchers worked on generating mathematic model leading to improve drilling performance. The first accurate geometry model and grinding principle for the conventional twist drill point was developed by Galloway [4]in 1957. A dozen years later, Fujii et al. [5] study on optimizing flute and flank contours based upon Galloway's work, but a comprehensive mathematic model was still missing. After that, Tsai and Wu [6] developed a

mathematical model that describes drill flank geometry including the conical, hyperbolical, and ellipsoidal. This study gave an accurate method to represent the quadratic drill geometry which enables the flank to be analyzed accurately and conveniently by computer. In 1983, Radhakrishnan [7]first derived the mathematical model of the planar split drill point. Fugelso [8]in 1990 improved the drill point geometry from a conventional straight-cutting-edge to a curved-cutting-edge by rotating the drill about its axes by angle ω before sharpening. This improvement solved the problem that the clearance angle was too small nearby the chisel edge, because of which it came to be widely applied in the future drilling processes. In 1999, Ren and Ni [9]evaluated drill cutting angles by deriving both flute and flank surface mathematic model, and conclude the relationship between drill point grinding parameters and geometric design parameters.

For automatic 3D modeling software, Vijayaraghavan [12] etc. developed an automated 3D model software based on geometry and manufacturing parameters, and it can be output with solid geometry format which can be meshed and analyzed in FEA software efficiently. Li e al. [13]presented a method to automatically measure the relief angle and rake angle of the standard twist drill based on a 3D model created by PRO/E.

The flute model used in this thesis is built by applying the work of Wang [15]. Based on this, this new mathematic model of conical drill point and automatic 3D modeling software can be developed.

1.6. Thesis Outline

Chapter 2 describes the mathematic model of the conical drill point and presents the relation between design parameters and grinding parameters. The integrated CAD/CAM twist drill modeling software is discussed in Chapter 3. Chapter 4 introduces CAD/CAM/CAE applications to predict the cutting performance of the designed twist drill. Chapter 5 concludes the research at the current stage and the potential work in the future.

Chapter 2.   The Mathematic Model of the Conical Drill Point

2.1. Conical Flank Surface Mathematic Model

2.1.1.   Drill coordinate system configuration

As shown in Fig. 2.1, $O_T - x_T y_T z_T$ is the tool axis system. The origin O_T is located at the top

point of the drill point. The drill axis is the z_T axis. The $+x_T$ direction is defined by the direction

heading from the origin to the outer with respect to the vector $\overrightarrow{O_T A'}$. The angle between $+x_T$

and $\overrightarrow{O_T A'}$ is μ and A' is the projection of the outer corner point A on the $x_T y_T$ plane. Then,

$+y_T$ can be specified by the right-hand rules according to the defined $+x_T$ and $+z_T$. The distance

between A' and A measured on z_T is t.
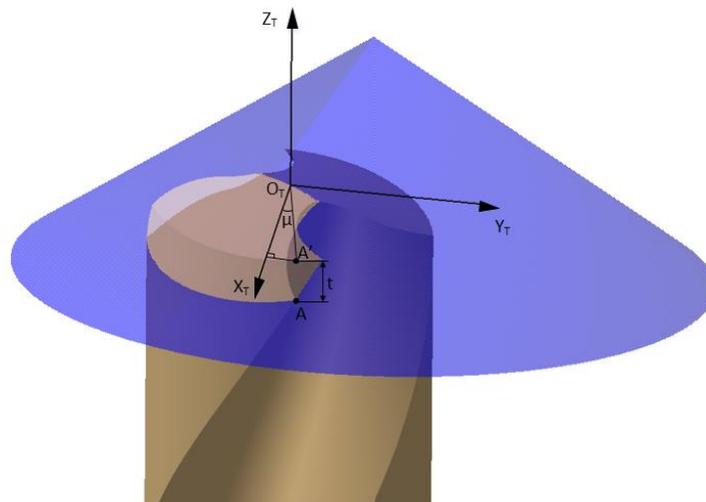
Figure 2.1 Configuration of drill axis system

2.1.2. Cone coordinate system configuration

The conical flank surface can be ground by two cone surfaces. Based on the grinding machine configuration, there are five grinding parameters involved:

1) Semi cone angle, θ

2) The angle rotated about y_T, σ

3) The distances translated along $x_T, y_T, z_T, a_x, a_y, a_z$.

As shown in Fig.2. 2, $O*-x*y*z*$ is the cone coordinate system. The angle between drill axis and cone axis is denoted as σ. The distance between cone axis and drill axis measured along y_T is a_y. Similarly, a_x and a_z are the projections of the distance between the origin of cone axis and drill axis on x_T and z_T, respectively.
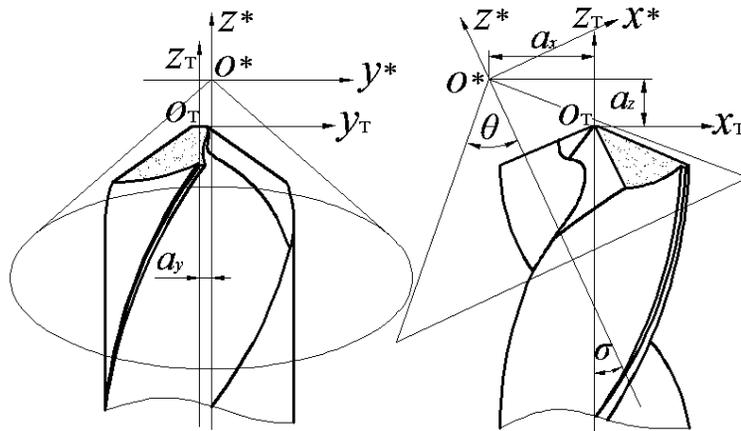
Figure 2.2 Cone axis system

2.1.3. Mathematic model of the conical flank surface

The conical surface expressed in the cone axis system $O^* - x^* y^* z^*$ is

$$x^{*2} + y^{*2} = z^{*2} \tan^2 \theta \tag{1}$$
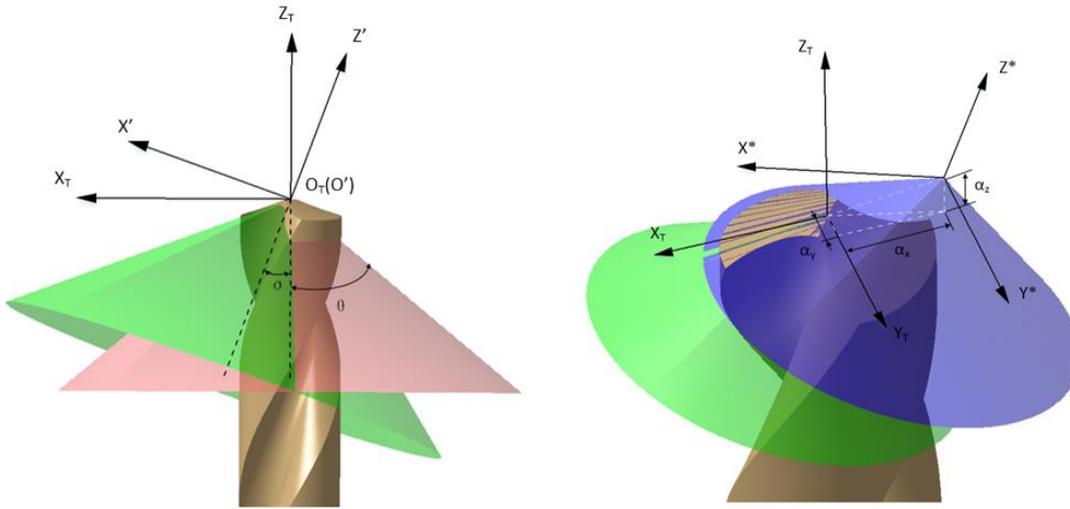
Figure 2.3 Coordinate translation

The cone surface can be translated onto drill axis system through these five grinding parameters. As shown in the Fig. 2.3, this converting procedure can be regarded as that first locating the cone at the tool coordinate system, and then rotating the translated cone about y_T by σ with reference to $+y_T$ in the clockwise. Finally, translating along x_T, y_T, z_T separately by $-a_x, a_y, a_z$.

This translation matrix is

$$T = T(z_T, a_z) \cdot T(y_T, a_y) \cdot T(x_T, -a_x) \cdot R(z_T, -\sigma)$$

$$= \begin{bmatrix} 1 & 0 & 0 & -a_x \\ 0 & 1 & 0 & a_y \\ 0 & 0 & 1 & a_z \\ 0 & 0 & 0 & 1 \end{bmatrix} \begin{bmatrix} \cos(-\sigma) & 0 & \sin(-\sigma) & 0 \\ 0 & 1 & 0 & 0 \\ -\sin(-\sigma) & 0 & \cos(-\sigma) & 0 \\ 0 & 0 & 0 & 1 \end{bmatrix}$$

$$= \begin{bmatrix} \cos\sigma & 0 & -\sin\sigma & -a_x \\ 0 & 1 & 0 & a_y \\ \sin\sigma & 0 & \cos\sigma & a_z \\ 0 & 0 & 0 & 1 \end{bmatrix} \tag{2}$$

The conical surface expressed in the tool axis system $O_T - x_T y_T z_T$ and the cone axis system

$O*-x*y*z*$ are denoted by C_T and $C*$, respectively. The relationship between C_T and

$C*$ can be represented as

$$C* = T^{-1} \cdot C_T$$

$$= \begin{bmatrix} \cos\sigma & 0 & \sin\sigma & a_x \cos\sigma - a_z \sin\sigma \\ 0 & 1 & 0 & -a_y \\ -\sin\sigma & 0 & \cos\sigma & -a_x \sin\sigma - a_z \cos\sigma \\ 0 & 0 & 0 & 1 \end{bmatrix} \begin{bmatrix} x_T \\ y_T \\ z_T \\ 1 \end{bmatrix}$$

$$= \begin{bmatrix} x_T \cos\sigma + z_T \sin\sigma + a_x \cos\sigma - a_z \sin\sigma \\ y_T - a_y \\ -x_T \sin\sigma + z_T \cos\sigma - a_x \sin\sigma - a_z \cos\sigma \\ 1 \end{bmatrix} \tag{3}$$

Substituting Eq. (3) into Eq. (1). The conical surface F_{C1} with respect to the drill coordinate

system $O_T - x_T y_T z_T$ can be derived as

$$(x_T \cos\sigma + z_T \sin\sigma + a_x \cos\sigma - a_z \sin\sigma)^2 + (y_T - a_y)^2$$
$$-(x_T \sin\sigma - z_T \cos\sigma + a_x \sin\sigma + a_z \cos\sigma)^2 \tan^2\theta = 0 \tag{4}$$

where $a_x > 0, a_z > 0$.

14

The another conical flank surface F_{C2} is

$$(-x_\mathrm{T} \cos\sigma + z_\mathrm{T} \sin\sigma + a_x \cos\sigma - a_z \sin\sigma)^2 + (-y_\mathrm{T} - a_y)^2$$
$$-(-x_\mathrm{T} \sin\sigma - z_\mathrm{T} \cos\sigma + a_x \sin\sigma + a_z \cos\sigma)^2 \tan^2\theta = 0 \tag{5}$$

where $a_x > 0, a_z > 0$.

Fig 2.4 shows the position and orientation of F_{C1} and F_{C2} in terms of drill coordinate system.

These two cone surfaces actually represent two separate conical flank surface.
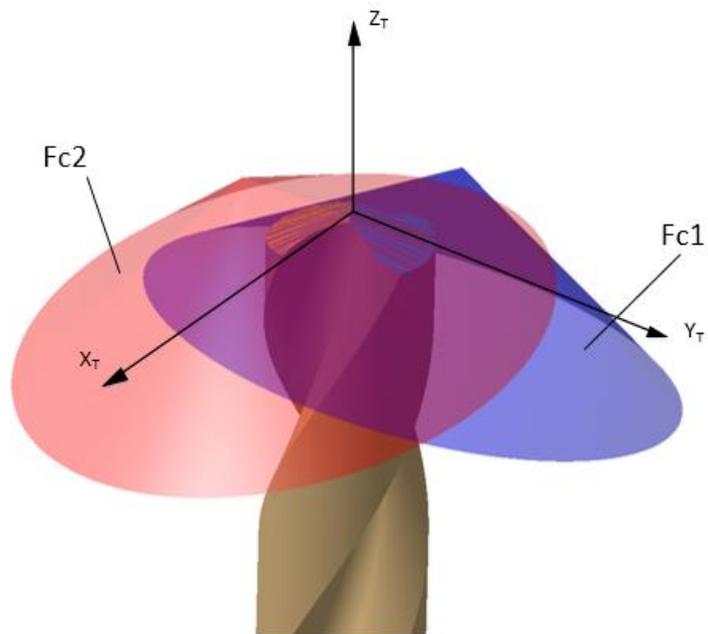
Figure 2.4 Fc1 and Fc2 in drill axis system

15

2.2. The Relationship Between Geometric Design and Grinding Parameters

Generally, a drill is designed in terms of its geometry parameters but manufactured on the basis of grinding parameters. Therefore, the corresponding relationship between the geometrical design parameters and the grinding parameters must be established to achieve the conversion between the two groups of parameters.

2.2.1. Relationship between chisel edge angle and grinding parameters

As shown in the Fig.2.5, chisel edge is the intersection of two cone surfaces. The mathematic model of conical flank surface is

$$\begin{cases} (x_T \cos\sigma + z_T \sin\sigma + a_x \cos\sigma - a_z \sin\sigma)^2 + (y_T - a_y)^2 - \\ (x_T \sin\sigma - z_T \cos\sigma + a_x \sin\sigma + a_z \cos\sigma)^2 \tan^2\theta = 0 \\ (-x_T \cos\sigma + z_T \sin\sigma + a_x \cos\sigma - a_z \sin\sigma)^2 + (-y_T - a_y)^2 - \\ (-x_T \sin\sigma - z_T \cos\sigma + a_x \sin\sigma + a_z \cos\sigma)^2 \tan^2\theta = 0 \end{cases} \tag{6}$$
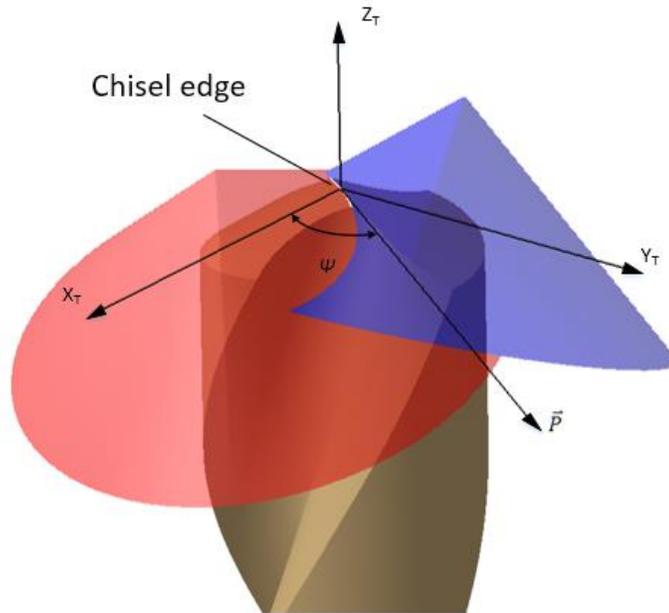
Figure 2.5 Chisel edge angle

16

Chisel edge angle is the acute angle between x_T and the tangent vector of the projection of chisel edge onto the plane $X_T Y_T$ at origin point of the drill axis system. The tangent vector is denoted by $\vec{P}$.

$$\vec{P} = \left[P_i, P_j, P_k \right] = \left[1, \frac{a_x \cos^2 \theta - a_x \sin^2 \sigma - a_z \sin \sigma \cos \sigma}{a_y \cos^2 \theta}, 0 \right] \tag{7}$$

Apparently, $\vec{P}$ is on XY plane. Thus, chisel edge angle ψ can be directly measured onto plane $X_T Y_T$ and expressed as

$$\tan \psi = \frac{P_j}{P_i} = \frac{a_x \cos^2 \theta - a_x \sin^2 \sigma - a_z \sin \sigma \cos \sigma}{a_y \cos^2 \theta} \tag{8}$$

2.2.2. Relationship between semi-point angle and grinding parameters

Semi-point angle is defined as the acute angle between the tangent of the projection of the cutting edge onto the structural plane $X_T Z_T$ at the outer corner point A and the drill axis Z_T. Geometrically, it can be easily detected from Fig. 2.6, cutting edge as an important feature of drill point is formed by flute contour and flank contour, which means that establishing an exact equation of point angle requires to build up flute mathematic model. However, in consideration of numerous of existing parameters may involved in the flute mathematic model, it definitely will bring a great complexity to express the cutting edge equation.

17
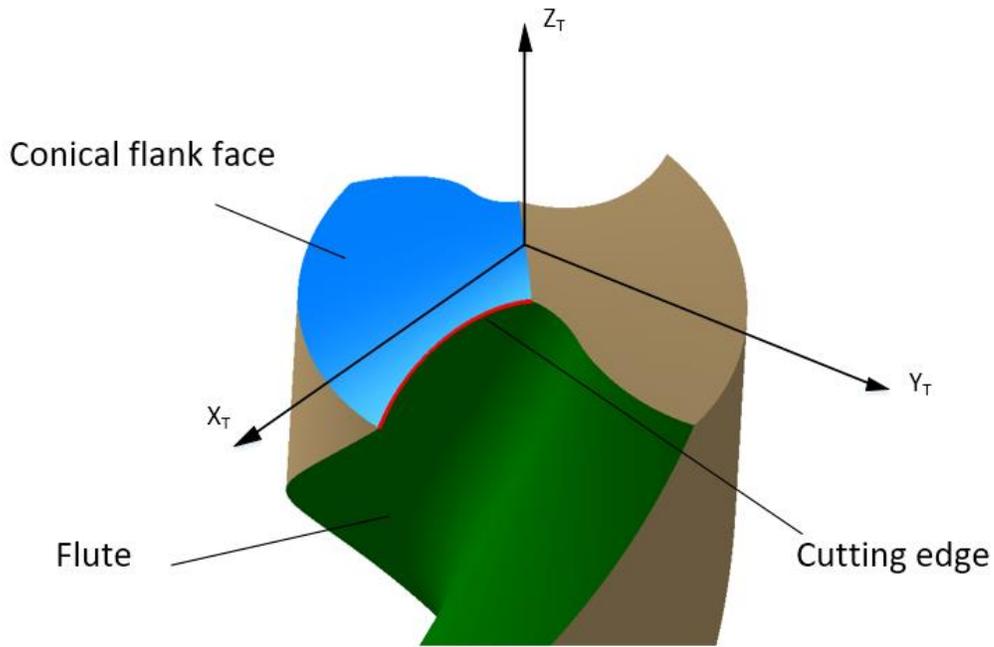
Figure 2.6 Cutting edge

To simplify the mathematic model, it is important to notice that the cutting edge projected on plane $X_T Z_T$ approaches a straight line which is similar with the line intersected by a plane and the conical surface. For this reason, the projection of the cutting edge in this paper is replaced by the intersection of the reference plane $y_T = r_c$ and conical flank surface, and semi-point angle can be redefined as the angle between the tangent of this intersection at the outer corner and the drill axis Z_T. See Fig.2.7.
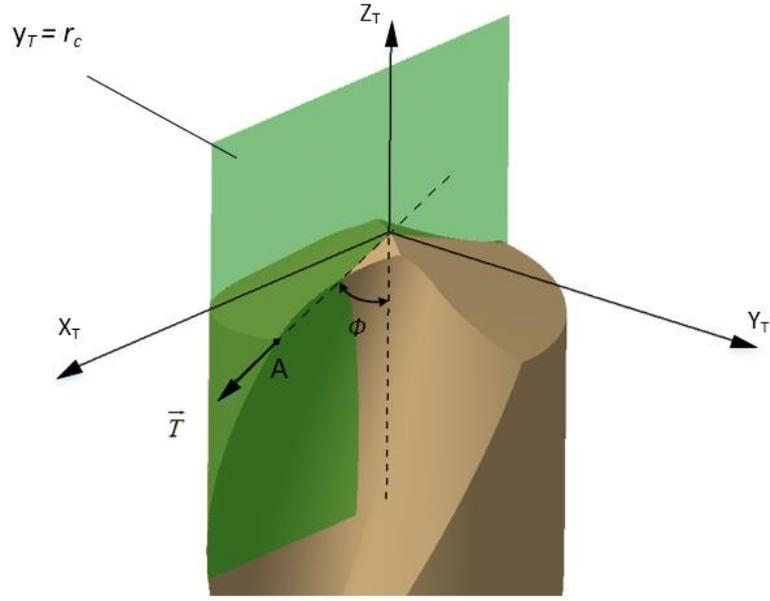
Figure 2.7 Semi point angle

The intersection of the reference plane $y_T = r_c$ and drill flank surface can be represented as

$$\begin{cases} (x_T \cos\sigma + z_T \sin\sigma + a_x \cos\sigma - a_z \sin\sigma)^2 + (y_T - a_y)^2 - \\ (x_T \sin\sigma - z_T \cos\sigma + a_x \sin\sigma + a_z \cos\sigma)^2 \tan^2\theta = 0 \\ y_T - r_c = 0 \end{cases} \tag{9}$$

Assume $\vec{T}$ is the tangent vector of the intersection of plane $Y_T = r_c$ and flank surface F_{C1} at outer corner, then

$$\vec{T} = \left[1, 0, -\frac{F_x}{F_z} \right] \tag{10}$$

where $F_x = \dfrac{\partial F_{C1}}{\partial x}$, $F_z = \dfrac{\partial F_{C1}}{\partial z}$.

Semi-point angle ϕ can be derived as

$$\tan\phi = -\frac{T_i}{T_k} = \frac{F_z}{F_x} \tag{11}$$

Assume the distance between outer corner A and plane $X_T Y_T$ is t. The distance measured from

outer corner A to the plane $X_T Z_T$ is r_c. Outer corner in drill coordinate system can be described

as $A(R\cos\mu, r_c, -t)$. The definition of μ is discussed in the previous section, it is easy to find the

relationship $\sin\mu = \frac{r_c}{R}$. Thus, the expression of the outer corner $A(R\cos\mu, R\sin\mu, -t)$ is derived.

Substituting it into equation (11)

$$\tan\phi = \frac{(-t - a_z)(\cos^2\theta - \cos^2\sigma) + (R\cos\mu + a_x)\sin\sigma\cos\sigma}{(R\cos\mu + a_x)(\cos^2\theta - \sin^2\sigma) + (-t - a_z)\sin\sigma\cos\sigma} \tag{12}$$

And t can be expressed as

$$t = -a_z + \cot\sigma(a_x + R\cos\mu) - \frac{a_x + R\cos\mu - a_x\cos^2\theta - a_y\cos^2\theta\cot\mu}{\cos\sigma\sin\sigma} \tag{13}$$

2.2.3. Relationship between lip relief angle and grinding parameters

A proper lip relief angle can reduce the heat generation and friction on the premise of

maintaining the strength of cutting lip while the drill point is thrusting in the material. To define

lip relief angle, it is very important to distinguish two definitions of lip relief angle: axial relief

angle and structural relief angle. These two parameters are both to describe the strength of

cutting lip structure, but measured on the different reference plane.

20

It is able to start with building a reference plane perpendicular to the radial direction of the drill at the outer corner *A*, and denote the mentioned reference plane as P_f. Similarly, we can also build a normal plane of the X_T in the drill axis system at the outer corner and name it as P_c. The intersection of the conical flank surface with each of two reference planes is a curve. We define the angle between the plane $X_T Y_T$ and the tangent of the intersected curve formed by P_c as axial relief angle, and the angle measured on P_f is structural relief angle. Normally, the definition of lip relief angle refers to structural relief angle, which is measured on the reference plane P_f. To solve the mathematic equation of structural relief angle in terms of drill axis system is complicated. In contrast, obtaining the expression of axial relief angle first and then converting the solved axial relief angle into structural relief angle seems to become a more skillful way.

Specifically, the axial relief angle is specified by creating a reference plane P_c parallel to the plane $Z_T Y_T$ at the outer corner A, and creating a tangent of the intersection of the flank surface and the created reference plane P_c. The angle between the tangent line and $X_T Y_T$ plane is the axial relief angle, denoted as α_c which is shown in Figure 2.8 .
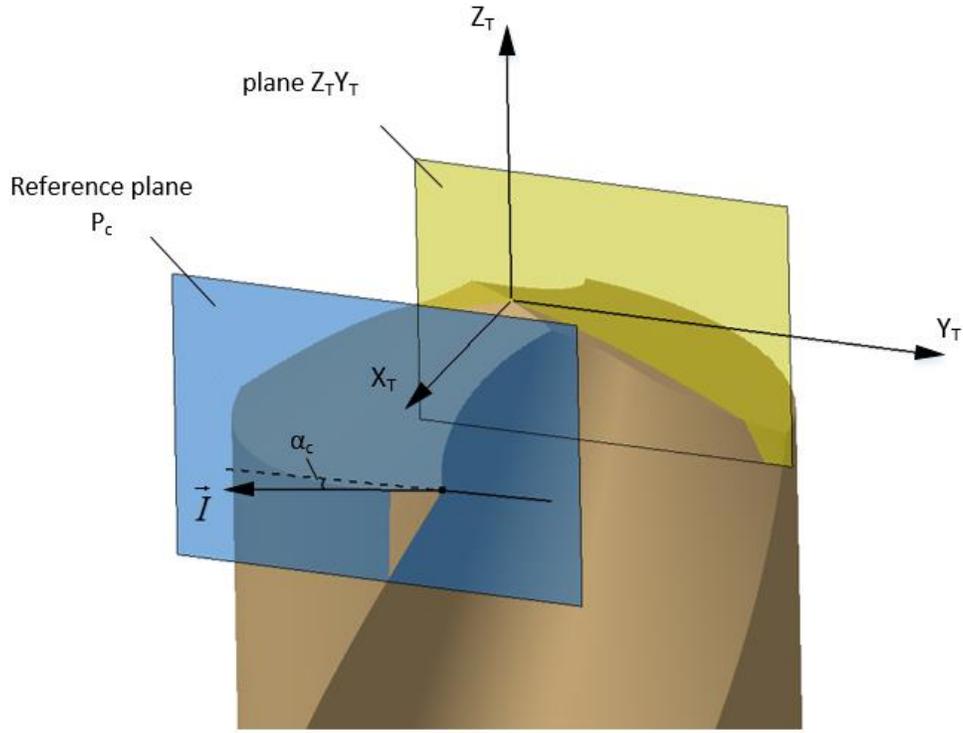
Figure 2.8 Axial relief angle α_c

The reference plane P_c is perpendicular to the axis X_T and passes through the outer corner A.

Therefore, the reference plane P_c can be derived as

$$X_T = R\cos\mu \tag{14}$$

And, the intersection of the P_c and the conical flank surface can be derived as

$$\begin{cases} (x_T\cos\sigma + z_T\sin\sigma + a_x\cos\sigma - a_z\sin\sigma)^2 + (y_T - a_y)^2 - \\ (x_T\sin\sigma - z_T\cos\sigma + a_x\sin\sigma + a_z\cos\sigma)^2 \tan^2\theta = 0 \\ X_T = R\cos\mu \end{cases} \tag{15}$$

The tangent vector $\vec{I}$ of the intersection at outer corner $A\,(R\cos\mu, R\sin\mu, -t)$ is

$$\vec{I} = \left[0, F_z, -F_y\right] \tag{16}$$

Where, $F_y = \dfrac{\partial F_{C1}}{\partial y}, F_z = \dfrac{\partial F_{C1}}{\partial z}$.

Geometrically, α_c can be derived as

$$\tan \alpha_c = -\frac{F_y}{F_z} \tag{17}$$

Substitute equation (13) into equation (17),

$$\tan \alpha_c = \frac{(a_y - R \sin \mu)(\sin \sigma \cos \sigma \tan \phi + \cos^2 \sigma - \cos^2 \theta)}{(a_x + R \cos \mu) \tan \phi \sin^2 \theta} \tag{18}$$

The structural relief angle α_f is measured on the reference plane P_f which is perpendicular to the radial direction of toolbar at the outer corner A. The structural relief angle α_f is the lip relief angle of the conical drill point. As shown in Fig. 2.10, the red reference plane is P_f where the structural relief angle α_f is measured. The blue plane P_c is the reference plane for axial relief angle α_c. White dash lines represent the projection elements of structural relief angle α_f from P_f onto P_c. $\vec{K}$ is the tangent of the intersection of the conical flank surface and P_f. $\vec{K}$ is the projection on P_c.
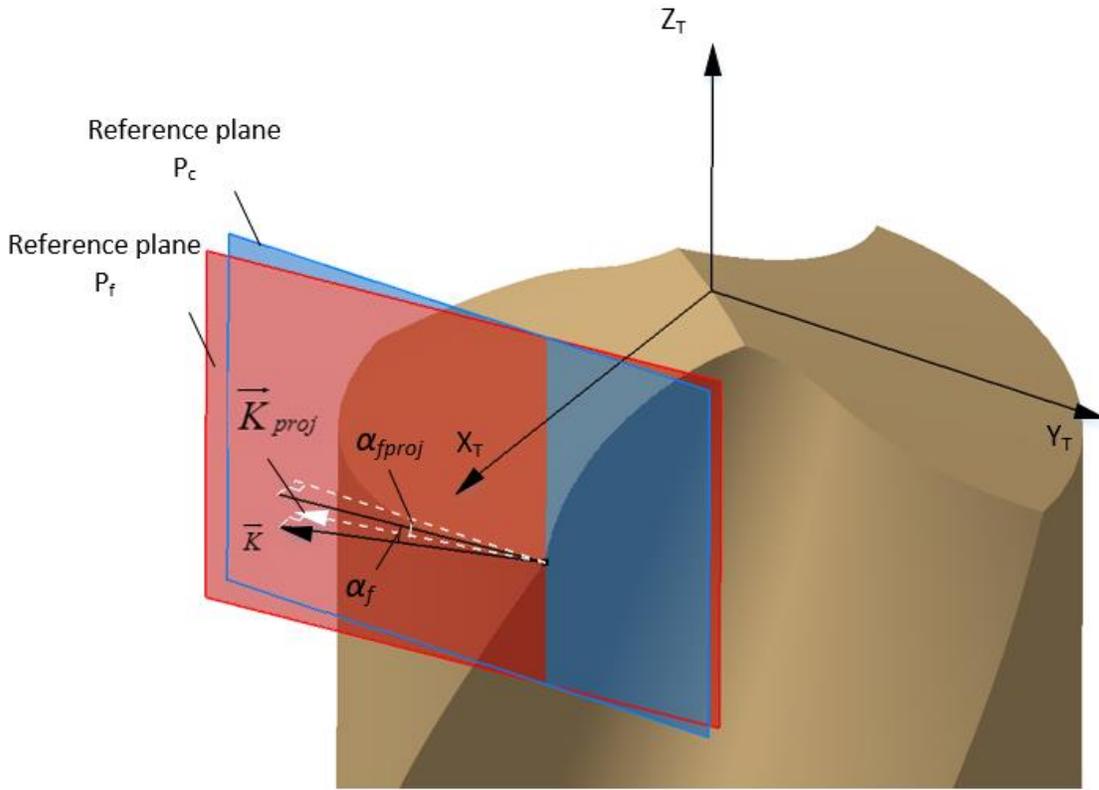
Figure 2.9 Structural relief angle

The reference plane P_f can be expressed as

$$x_T \cos \mu + y_T \sin \mu - R = 0 \tag{19}$$

The intersection of P_f and flank surface is

$$\begin{cases} (x_T \cos \sigma + z_T \sin \sigma + a_x \cos \sigma - a_z \sin \sigma)^2 + (y_T - a_y)^2 - \\ (x_T \sin \sigma - z_T \cos \sigma + a_x \sin \sigma + a_z \cos \sigma)^2 \tan^2 \theta = 0 \\ x_T \cos \mu + y_T \sin \mu - R = 0 \end{cases} \tag{20}$$

The tangent of the intersection is

$$\vec{K} = \left[-F_z G_y, F_z G_x, F_x G_y - G_x F_y \right] \tag{21}$$

Project $\vec{K}$ on reference plane P_c, the projection $\vec{K}_{proj}$ is

$$\vec{K}_{proj} = \left[0, F_z G_x, F_x G_y - G_x F_y \right] \tag{22}$$

The angle $\alpha_{f_{proj}}$ is the angle between $\vec{K}_{proj}$ and the vertical projection on $X_T Y_T$ plane, measured on P_c plane, which is

$$\tan \alpha_{f_{proj}} = \frac{F_x G_y - G_x F_y}{F_z G_x} \tag{23}$$

Integrating equation (11) and equation (17) into equation (23), the $\alpha_{f_{proj}}$ can be derived as

$$\tan \alpha_{f_{proj}} = \frac{\tan \mu}{\tan \phi} + \tan \alpha_c \tag{24}$$

The relationship between $\alpha_{f_{proj}}$ and α_c is obtained. As mentioned above, $\alpha_{f_{proj}}$ is measured by projecting α_f from P_f onto P_c. P_f is perpendicular to the connection from origin to the outer corner's projection A', P_c is the normal plane of X_T intersecting P_f at outer corner A. μ is the angle between $+x_T$ and $\overrightarrow{O_T A'}$ which is explained in the previous chapter. It is not hard to deduce that the angle between P_f and P_c is μ as well. It shows in Fig. 2.10.
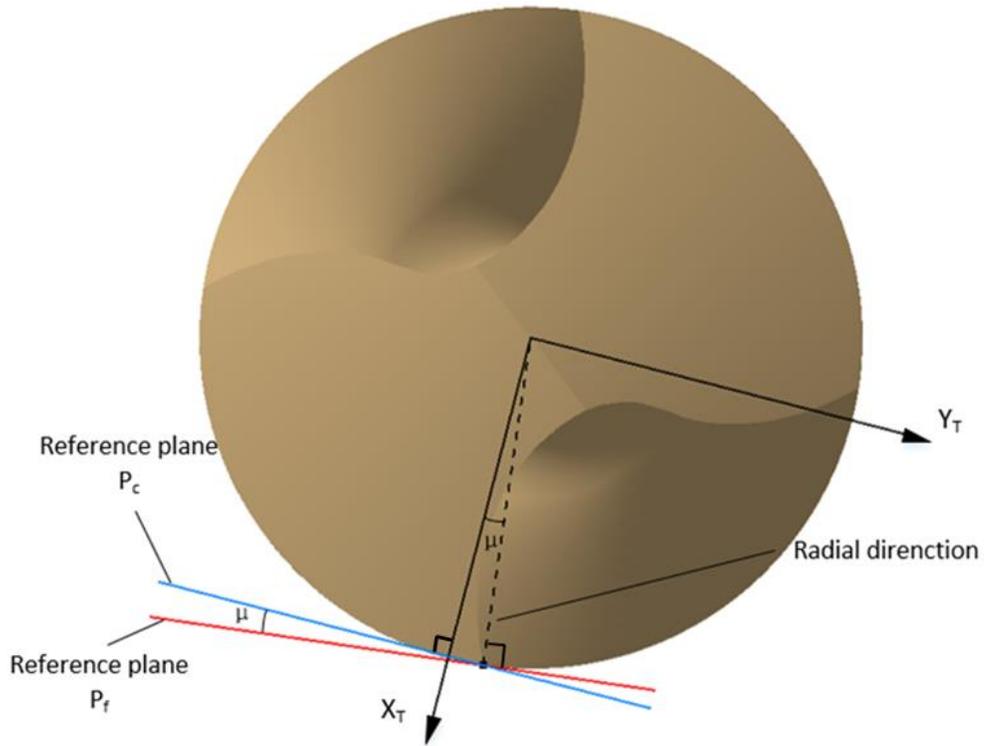
Figure 2.10 Relationship between P_c **and** P_f

Therefore, the relationship between $\alpha_{f_{proj}}$ and α_f is

$$ \tag{25} $$

Substituting equation (25) into equation (24), the converting relationship between α_c and α_f is deduced as,

$$ \tan\alpha_c = \frac{\tan\alpha_f}{\cos\mu} - \frac{\tan\mu}{\tan\phi} \tag{26} $$

2.3. Effect of Grinding Parameters on Design Parameters

2.3.1. Effect of grinding parameters on chisel edge angle

The relationship between grinding parameters and chisel edge angle implied in Equation (8) can

be displayed in Fig. 2.11. The chisel edge angle will increase with the rise of a_x but decrease

with the increasing of a_y, a_z, σ, θ. The parameter t has no effect on chisel edge angle.
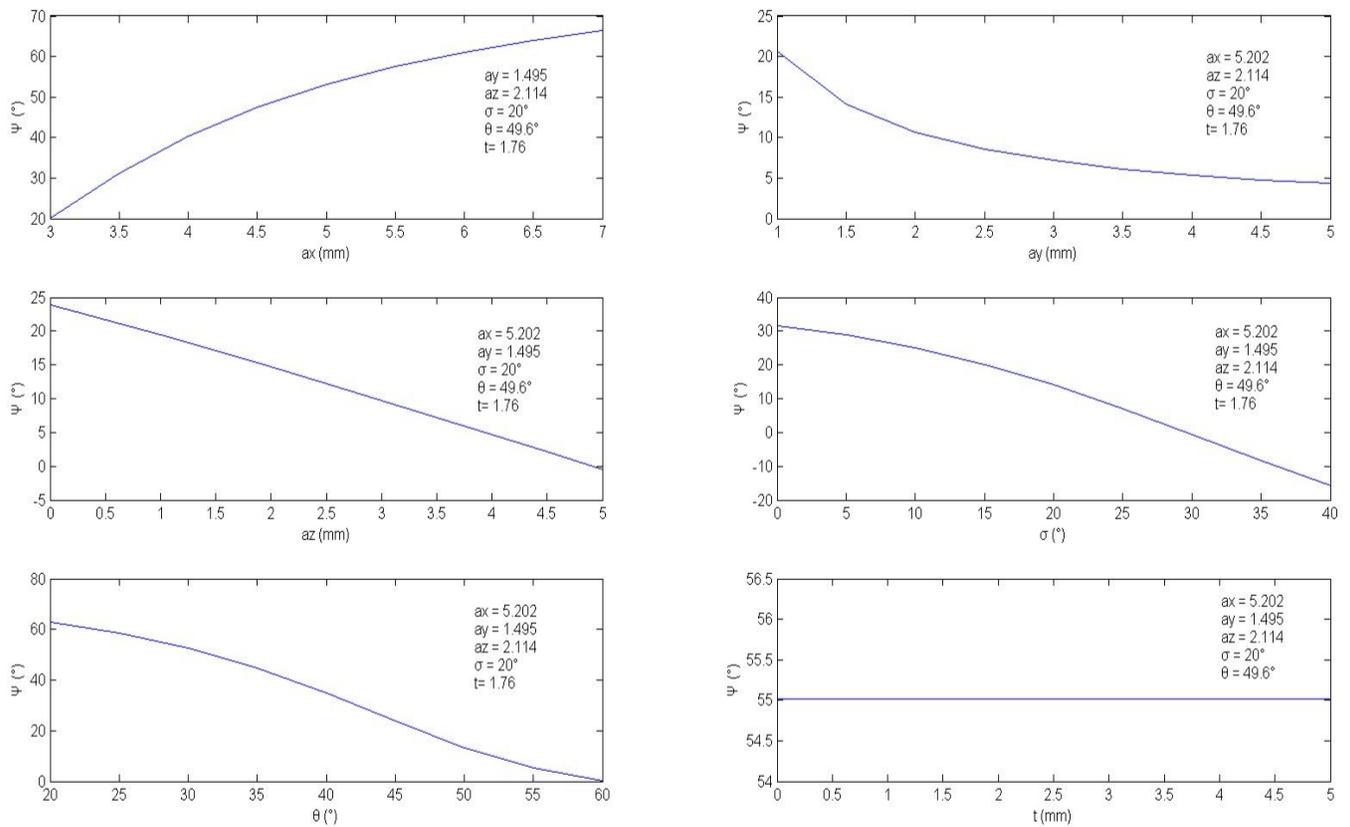
Figure 2.11 Effects of grinding parameters on chisel edge angle Ψ

2.3.2. Effects of grinding parameters on semi-point angle

Fig.2.12 shows that the effect of grinding parameters on semi point angle that is indicated in equation (12). The drill diameter D = 10mm, and r_c = 0.1. a_x is the only parameter results in the decreasing of semi point angle. a_y does not affect semi point angle. For the rest of grinding parameters, they all bring the growth to semi point angle in various degree.
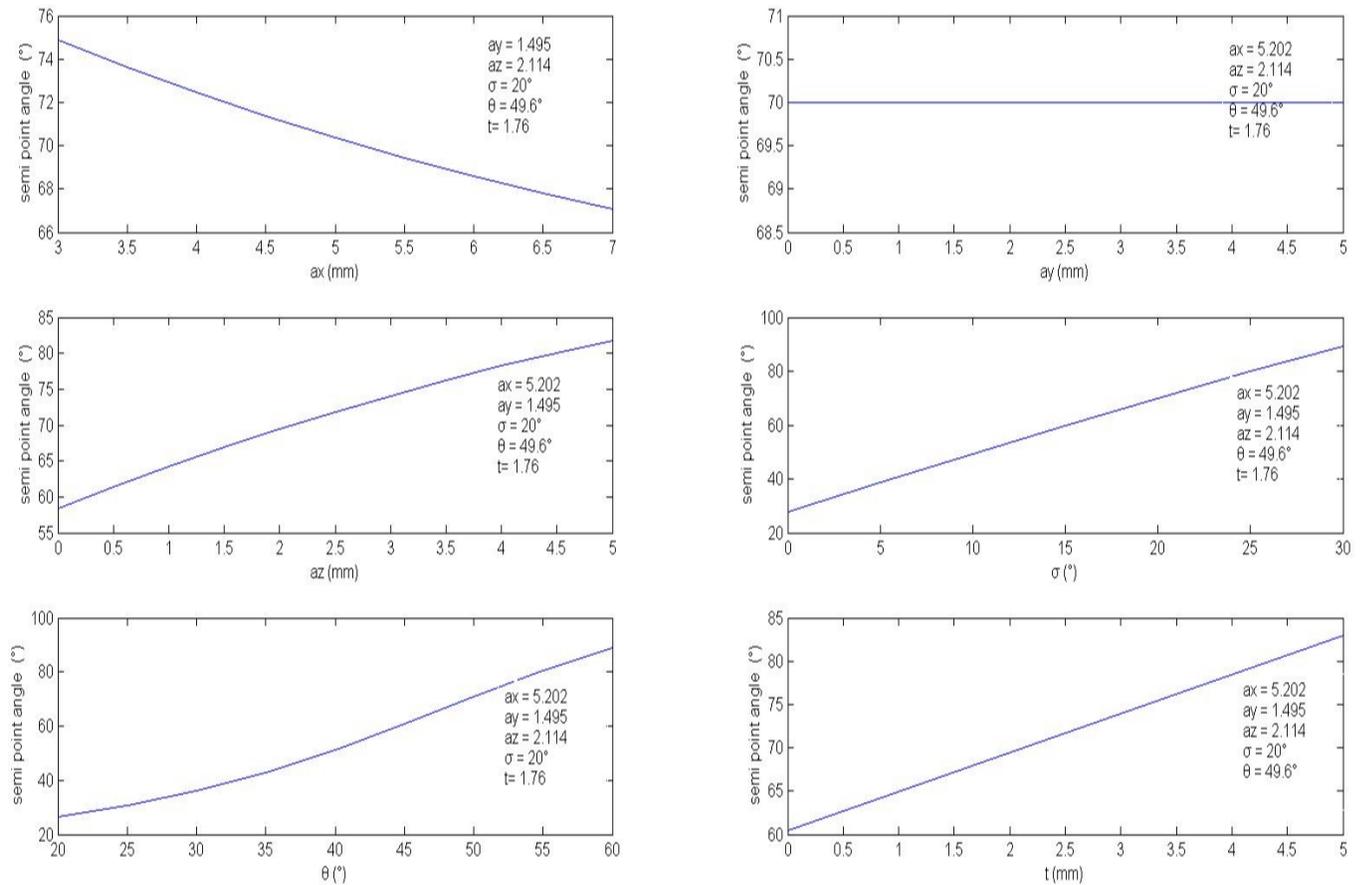
Figure 2.12 Effects of grinding parameters on semi point angle Φ

2.3.3. Effects of grinding parameters on lip relief angle

According to Equation (18), the effect of grinding parameters on lip relief angle can be graphically illustrated in Fig.2.13, lip relief angle decreases with the increasing of a_y, but $a_x, a_z, \sigma, \theta, t$ provide opposite influence.
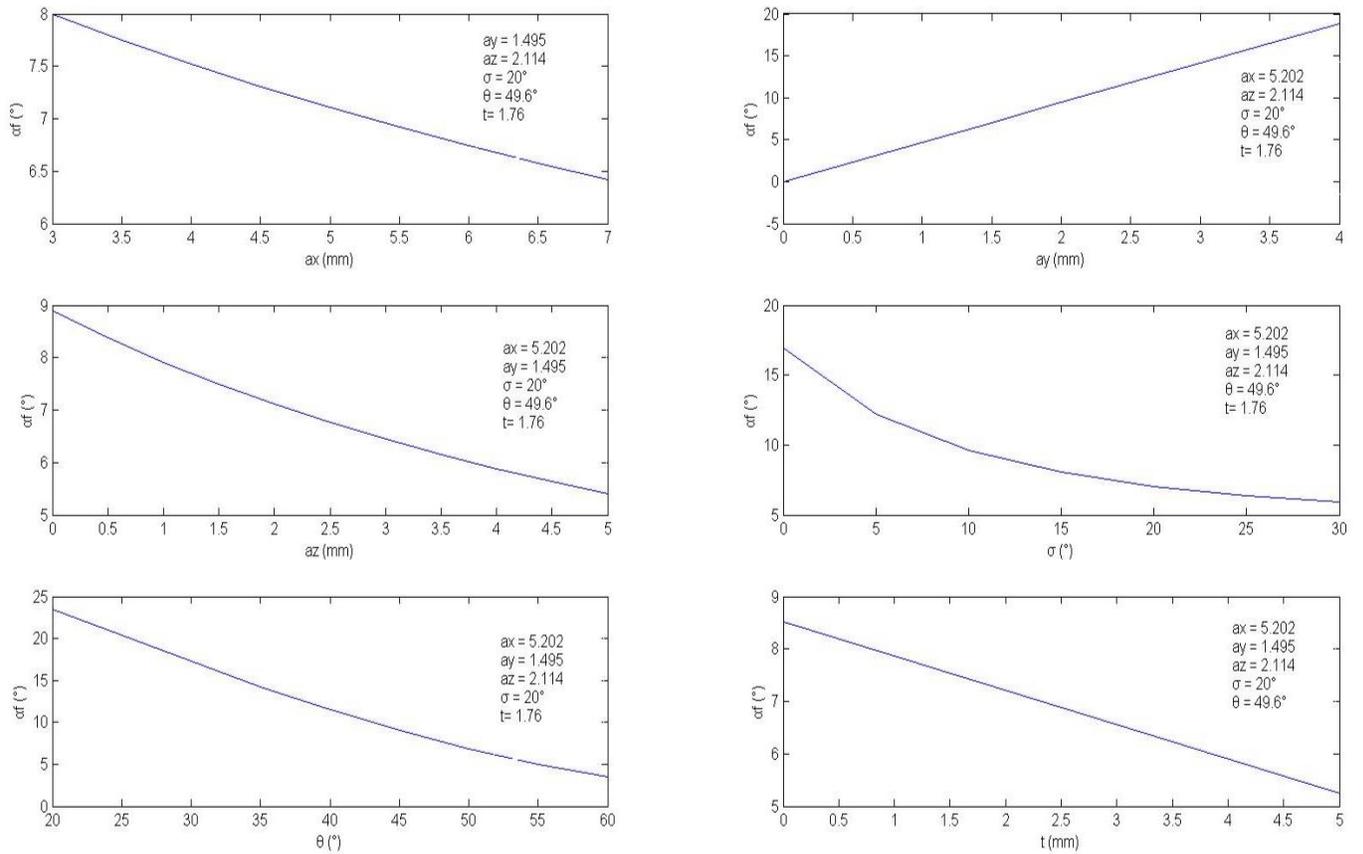
Figure 2.13 Effects of grinding parameters on lip relief angle αf

2.4. Solution for Grinding Parameters

As mentioned in the previous content, we cannot build a 3D model and calculate grinding path without knowing grinding parameters. However, before we starting to build a model, the known condition is normally a group of design parameters which are really limited and delivered only on a piece of 2D drawing. Thus, to derive the solution for grinding parameters based on relative design parameters comes to an essential task.

As can be seen in Fig.2.14. The conical point mathematic model can be regarded as a black box with the input of groups of design parameters (Ψ, Φ, α_f), setting up parameters (σ, r_c) and the radius of the drill (R). If it meets the validation ($\Delta \geq 0$) while solving equations, the mathematic model outputs grinding parameters in terms of given design parameters. Otherwise, the designer has to think about the feasibility of the design and adjust design parameters until it meets the condition.
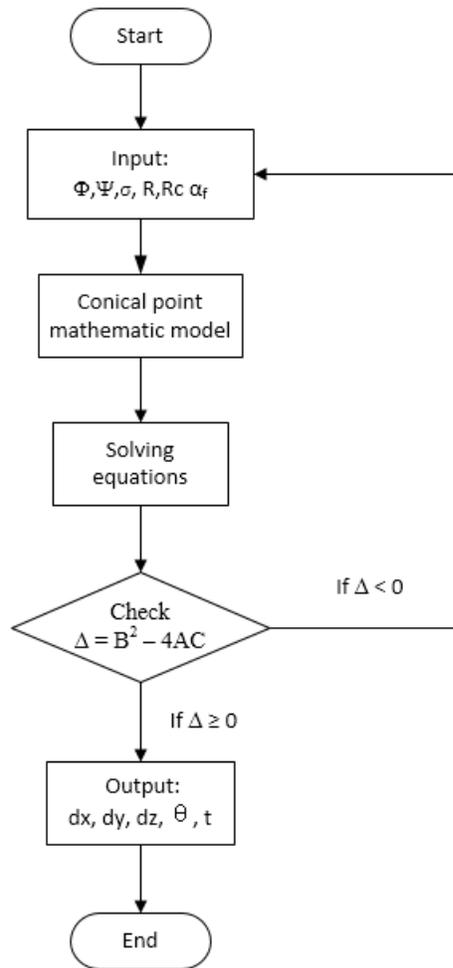
Figure 2.14 Flowchart of solving equations of conical point mathematic model

2.4.1. Solution for semi-cone angle θ

Geometrically, the cutting edge is specified by the flute shape and the cone surface and the outer

corner is the outermost point on the cutting edge. Thus, one of the crucial condition is that the

outer corner $A(R\cos\mu, R\sin\mu, -t)$ should locate on the cone surface. We can easily substitute

$A(R\cos\mu, R\sin\mu, -t)$ into the equation of the conical surface and derive this condition by the

following equation:

31

$$[R\cos\mu\cos\sigma + a_x\cos\sigma - (t+a_z)\sin\sigma]^2 + (R\sin\mu - a_y)^2 -$$
$$[R\cos\mu\sin\sigma + a_x\sin\sigma + (t+a_z)\cos\sigma]^2\tan^2\theta = 0 \tag{27}$$

To remove t, substituting equation (13) into equation (27),

$$(\sec^2\phi\sin^2\theta - \sin^2\sigma - \tan^2\phi\cos^2\sigma + 2\tan\phi\sin\sigma\cos\sigma)(R\cos\mu + a_x)^2$$
$$\sin^2\theta + (a_y - R\sin\mu)(\sin\sigma\cos\sigma\tan\phi + \cos^2\sigma - \cos^2\theta) = 0 \tag{28}$$

Continuing to substitute equation (18) into equation (28)

$$(\tan^2\phi\tan^2\alpha_c\cos^2\mu\sin^2\theta + \sec^2\phi\sin^2\theta - \sin^2\sigma -$$
$$\tan^2\phi\cos^2\sigma + 2\tan\phi\sin\sigma\cos\sigma)(R\cos\mu + a_x)^2 = 0 \tag{29}$$

Due to $R\cos\mu + a_x \neq 0$, semi point angle in terms of σ, ϕ, α_c can be solved as

$$\sin\theta = \sqrt{\frac{\sin^2\sigma + \tan^2\phi\cos^2\sigma - 2\tan\phi\sin\sigma\cos\sigma}{\tan^2\alpha_c\tan^2\phi\cos^2\mu + \sec^2\phi}} \tag{30}$$

2.4.2. Solution for a_x, a_y, a_z

According to another crucial condition for grinding the twist drill point, the cone has to pass the origin of the drill coordinate system. This condition can be derived as

$$(a_x\cos\sigma - a_z\sin\sigma)^2 + a_y^2 - (a_x\sin\sigma + a_z\cos\sigma)^2\tan^2\theta = 0 \tag{31}$$

Combined with equation (8), (12), (30) and (31), we can get

32

$$\begin{cases} \tan\psi = \dfrac{a_x \cos^2\theta - a_x \sin^2\sigma - a_z \sin\sigma\cos\sigma}{a_y \cos^2\theta} \\[4mm] \tan\alpha_c = \dfrac{(a_y - R\sin\mu)(\sin\sigma\cos\sigma\tan\phi + \cos^2\sigma - \cos^2\theta)}{(a_x + R\cos\mu)\tan\phi\sin^2\theta} \\[4mm] (a_x\cos\sigma - a_z\sin\sigma)^2 + a_y^2 - (a_x\sin\sigma + a_z\cos\sigma)^2\tan^2\theta = 0 \end{cases} \qquad (32)$$

According to equation (12), it is easy to express a_y by a_x as

$$a_y = P_1 a_x + P_2 \qquad (33)$$

Where

$$\begin{cases} P_1 = \dfrac{\tan\alpha_c \tan\phi\sin^2\theta}{\sin\sigma\cos\sigma\tan\phi + \cos^2\sigma - \cos^2\theta} \\[4mm] P_2 = P_1 R\cos\mu + R\sin\mu \end{cases} \qquad (34)$$

Substitute equation (33) into (8), a_z can also be presented by a_x,

$$a_z = P_3 a_x + P_4 \qquad (35)$$

Where

$$\begin{cases} P_3 = \dfrac{\cos^2\theta - \sin^2\sigma - P_1\cos^2\theta\tan\psi}{\sin\sigma\cos\sigma} \\[4mm] P_4 = -\dfrac{(P_1 R\cos\mu + R\sin\mu)\cos^2\theta\tan\psi}{\sin\sigma\cos\sigma} \end{cases} \qquad (36)$$

Integrating equation (33) and (35) into equation (31), we can obtain

$$A a_x^2 + B a_x + C = 0 \qquad (37)$$

And a_x can be expressed as

33

$$a_x = \frac{-2B \pm \sqrt{B^2 - 4AC}}{2A} \qquad (38)$$

However, based on the practical engineering experience, a_x should be expressed as

$$a_x = \frac{-2B - \sqrt{B^2 - 4AC}}{2A} \qquad (39)$$

Where

$$\begin{cases} A = (\cos\sigma - P_3\sin\sigma)^2 - (\sin\sigma + P_3\cos\sigma)^2\tan^2\theta + P_1^2 \\ B = -2[P_4(\cos\sigma - P_3\sin\sigma)\sin\sigma + P_4(\sin\sigma + P_3\cos\sigma)\cos\sigma\tan^2\theta - P_1P_2] \\ C = P_4^2 + P_2^2 - P_4^2\cos^2\sigma\sec^2\theta \end{cases} \qquad (40)$$

It should be noted that σ affects the degree of the curvature of the flank surface, which is supposed to be specified by different machining demands. Generally, a greater σ means a greater curvature of the flank surface. According to the practical design requirement, σ can be fixed in advance. Therefore, all equations can be solved.

$$\begin{cases} a_x(\psi,\phi,\alpha_c) = \dfrac{-2B - \sqrt{B^2 - 4AC}}{2A} \\ a_y(\psi,\phi,\alpha_c) = \dfrac{-2B - \sqrt{B^2 - 4AC}}{2A}P_1 + P_2 \\ a_z(\psi,\phi,\alpha_c) = \dfrac{-2B - \sqrt{B^2 - 4AC}}{2A}P_3 + P_4 \end{cases} \qquad (41)$$

where

34

$$
\begin{cases}
A = (\cos\sigma - P_3\sin\sigma)^2 - (\sin\sigma + P_3\cos\sigma)^2\tan^2\theta + P_1^2 \\
B = -2[P_4(\cos\sigma - P_3\sin\sigma)\sin\sigma + P_4(\sin\sigma + P_3\cos\sigma)\cos\sigma\tan^2\theta - P_1P_2] \\
C = P_4^2 + P_2^2 - P_4^2\cos^2\sigma\sec^2\theta \\
P_1 = \dfrac{\tan\alpha_c\tan\phi\sin^2\theta}{\sin\sigma\cos\sigma\tan\phi + \cos^2\sigma - \cos^2\theta} \\
P_2 = P_1 R\cos\mu + R\sin\mu \\
P_3 = \dfrac{\cos^2\theta - \sin^2\sigma - P_1\cos^2\theta\tan\psi}{\sin\sigma\cos\sigma} \\
P_4 = -\dfrac{(P_1 R\cos\mu + R\sin\mu)\cos^2\theta\tan\psi}{\sin\sigma\cos\sigma}
\end{cases}
\tag{42}
$$

2.4.3. Solution for t

The parameter t is the distance between the outer corner and XY plane measured along drill axis. As discussed above, all necessary parameters have been given or solved. Based on equation (13), we can easily calculate the value of parameter t.

So far, by specifying the parameter σ according to the engineering experience and μ for establishing coordinate system. All grinding parameters should be available to be solved and expressed by design parameters.

2.5. Verification

Based on derived mathematic model above, a group of 4 different designs on conical drill point are developed to evaluate the accuracy and feasibility of the proposed method. The first group of design parameters are determined as the standard (chisel edge angle $\psi = 55°$, semi point angle $\phi = 70°$, and lip relief angle $\alpha_f = 7°$) , which are provided by a manufacturing supplier. For

35

the rest of designed samples, the involved parameters are specified by fixing two of design parameters and only modifying only one of them on each sample. Eventually, only one design parameter will be adjusted compared to the original group. It helps to clearly estimate every mathematic model of each design parameter. In these four designs, θ is fixed as 25° and r_c is specified as 0.1 according to the engineering experience. The corresponding 3D models of each group are simulated in CATIA and all the testing design parameters are measured on generated 3D models and compared with required design parameters.

The design parameters measured on CATIA 3D models can be achieved by "*measure*" function provided by CATIA. Fig.2.15 (a), (b), (c), (d) clearly illustrates generated 3D models of each group in different views. Every measured angle is highlighted by black solid line and the measured value is denoted in the green text box.

As can be seen in table 4-1, the first group experiment is regarded as a standard group where the data ($\psi = 55°, \phi = 70°, \alpha_f = 7°$) is determined by the dimensions of a twist drill used for drilling regular stainless steel. Parameters measured on the 3D model in CATIA is highly close to the required design parameters. In order to test the reliability and availability of the derived mathematic model, chisel edge angle, semi-point angle and lip relief angle are separately changed to $\psi = 40°, \phi = 60°, \alpha_f = 12°$ and corresponding 3D models are also built for the following three experiment group. Through these experiments, it is clearly to see that only a little difference can be found between the required design parameters and the ones measured on the 3D model. This verification proves the reliability of the proposed mathematic model of the conical drill point.

Table 2-1 Verification of five generated models

No.	Required design parameters (ψ, ϕ, α_f)	Measured design parameters $(\psi_m, \phi_m, \alpha_{fm})$	Difference $(\Delta\psi, \Delta\phi, \Delta\alpha_f)$
1	(55 ,70 ,7)	(55.005, 70.154, 7.345)	(0.005, 0.154, 0.345)
2	(55, 70, 12)	(55.004, 70.013, 11.988)	(0.004, 0.013, 0.012)
3	(40, 70, 7)	(40.001, 69.999, 6.997)	(0.001, 0.001, 0.03)
4	(55, 60, 7)	(54.994, 60.000, 7.002)	(0.006, 0, 0.002)
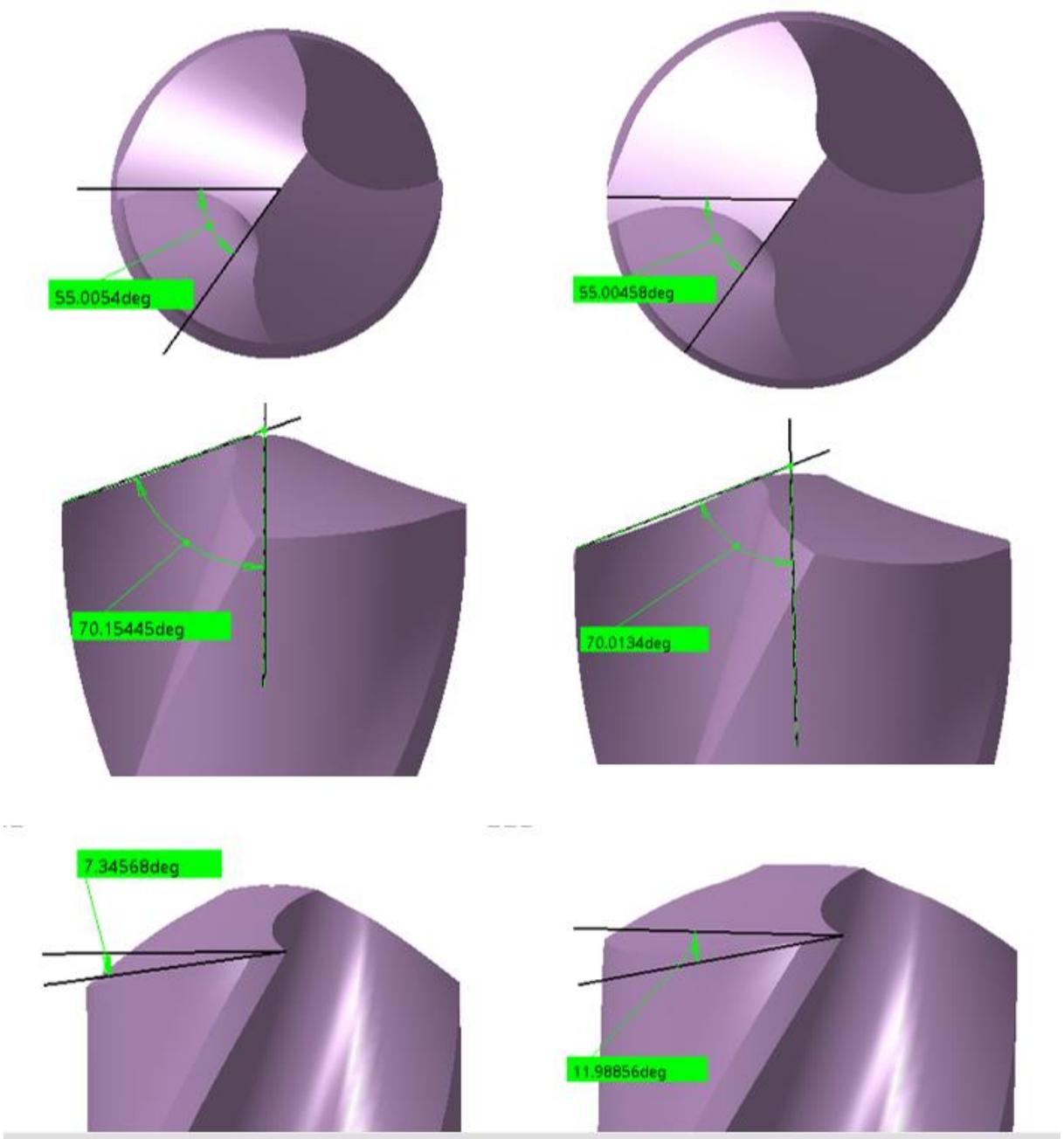
(a) Sample 1($\psi = 55°, \phi = 70°, \alpha_f = 7°$)   (b) Sample 2($\psi = 55°, \phi = 70°, \alpha_f = 12°$)
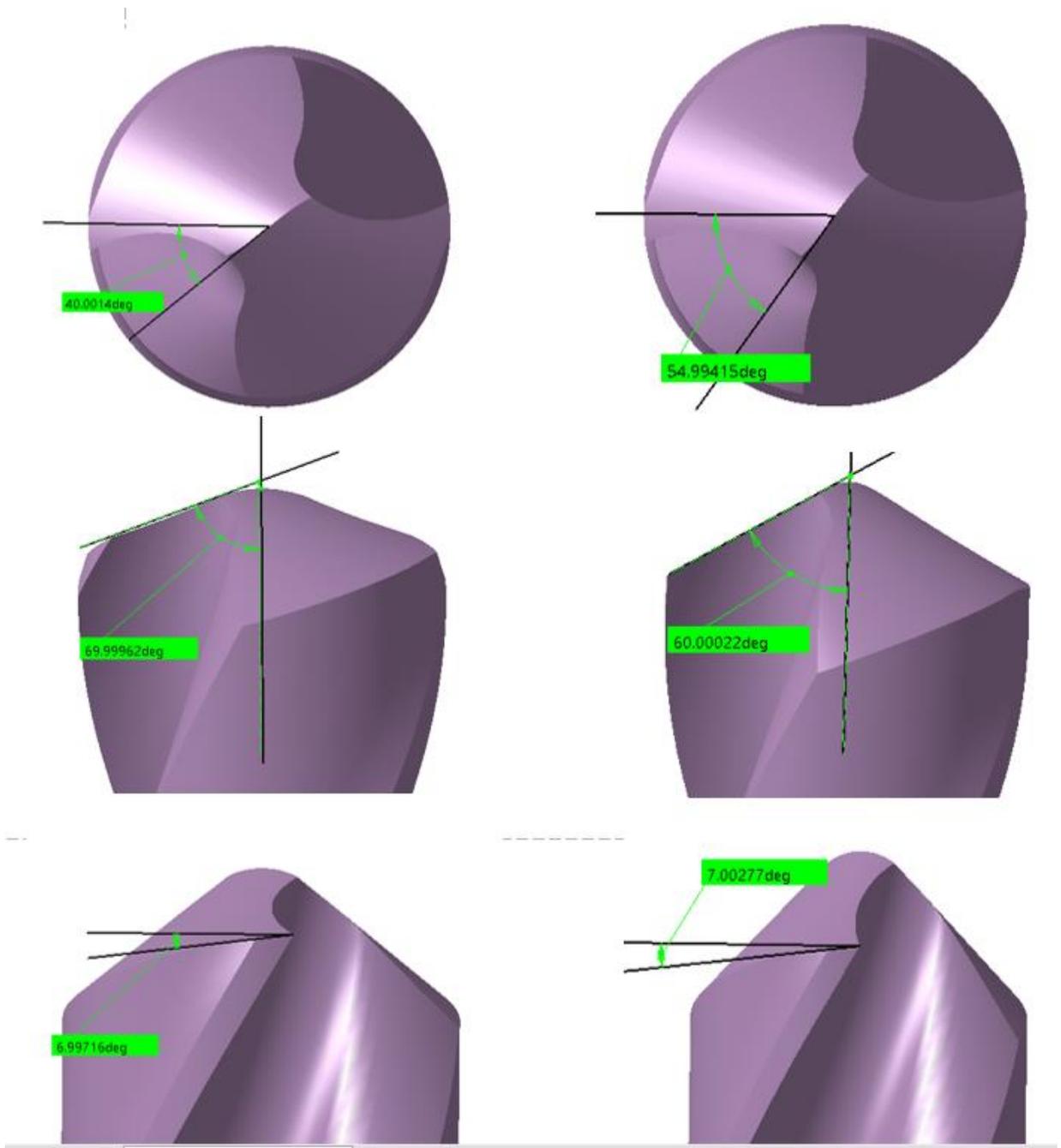
(d) Sample 3($\psi = 40°, \phi = 70°, \alpha_f = 7°$)　　　　(c) Sample 4($\psi = 55°, \phi = 60°, \alpha_f = 7°$)

Figure 2.15 Measured parameters on 3D models in CATIA

Chapter 3.   Integrated CAD/CAM Software

The software is used for offering a user-friendly interface to clearly instruct the user to design a twist drill in a correct order and output relative manufacturing information. Once the user defines all the details to the CNC machine, grinding wheel and the structure of a twist drill, this software can call the well-programmed m files to calculate the grinding parameter and grinding path. After that, CATIA can automatically build the 3D model based on the calculated result and the grinding path used for manufacturing each feature can be generated as well.

The greatest function of this software is modeling automation. This function can be achieved with the benefit of CATIA automation and macro programming technique. CATIA V5 automation was originally designed for VB6, VBA, and VBScript. Currently, Microsoft no longer officially supports VB6 as it has been replaced by VB.net. VB.net cannot only support all programming grammar for CATIA automation but also gives a great help to develop a good-looking interface.

3.1. Introduction

The software provides three separate workbenches: machining tool workbench, grinding wheel workbench and cutting tool workbench. The program logic of this software can be seen in Fig 3.1. It can be simply described that the user first selects a type of machining tool as the one used for the grinding process, next the user selects a kind of grinding wheel with defined dimensions and installs on the spindle of the selected machining tool. Finally, through inputting design parameters to each feature of the twist drill, the 3D modeling and grinding path of the designed twist drill can be generated.
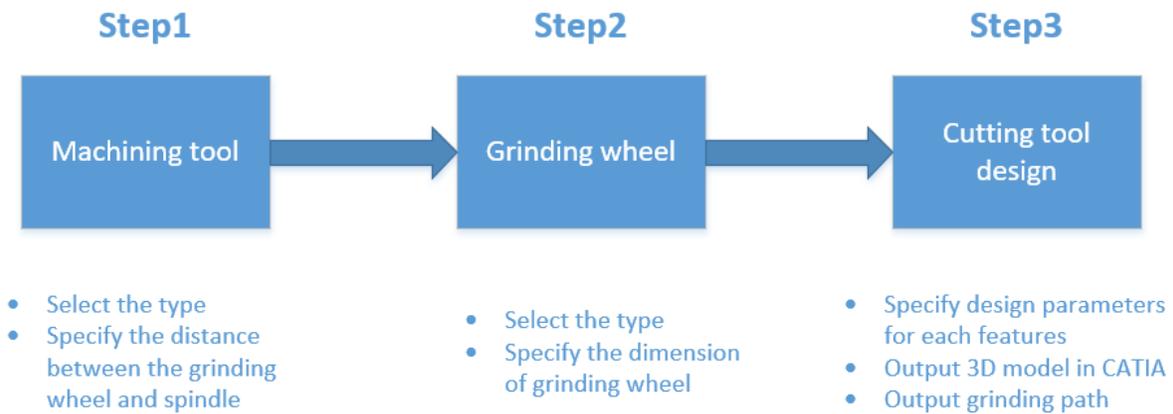
Figure 3.1 The program logic of the integrated CAD/CAM software

3.2. Machining Tool Workbench

This workbench is used for setting up basic parameters of the selected 5-axis grinding machine and preparing to output grinding path for each feature of the designed twist drill. Water Helitronic Essential is the 5-axis grinding tool used in this software, as shown in Fig.3.2. All the following grinding path is generated through the configuration of this grinding machine. Walter five-axis grinding machines are NC machines which characterized by three translational and two rotary axes. The whole machine can be generally divided into two parts. The upper parts can support the motion along Z and Y axes and connects the spindle 1 and spindle 2 on each side where grinding wheels can be loaded. The lower part is able to rotate around A axis and C axis and linear translate along X axis. A and C axes are the angular direction around X axis and Z axis, respectively. At the very beginning, a toolbar to be machined is put into the main spindle of the lower part by means of the clamping device, and several grinding wheels are fixed to two spindles on each side on the upper part. The toolbar is machined by moving the grinding wheel

41

along a pre-computed path in space called the grinding path. The grinding path will be computed

by CNC mathematic model and converted into G-code with the help of post processor. The

converted G-code is the programming language that could be recognized by CNC machine. In

this way, CNC machine could instruct the mounted grinding wheel to work along the required

grinding path.
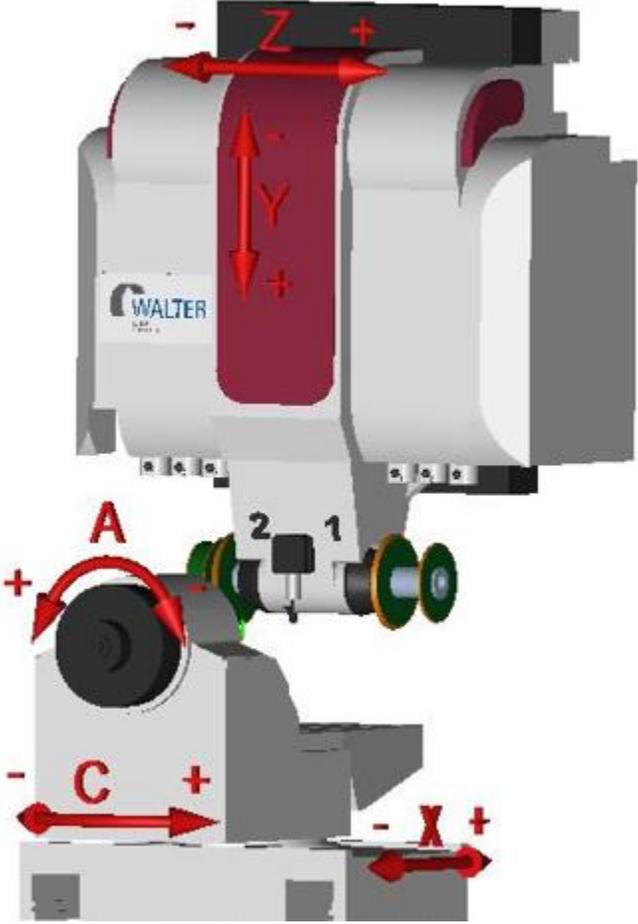
Figure 3.2 Walter 5-axis grinding machine

As shown in Fig.3.3, the machining tool workbench is used mainly for constraining the relative

relationship between installed grinding wheels and clamped toolbar. The important note is that

the grinding wheel located on spindle 1 can only grind the toolbar when C axis is in the positive

direction. Similarly, when the lower part rotates to the left side (negative angle in C direction), the toolbar can only be machined by the grinding wheel mounted on spindle 2.
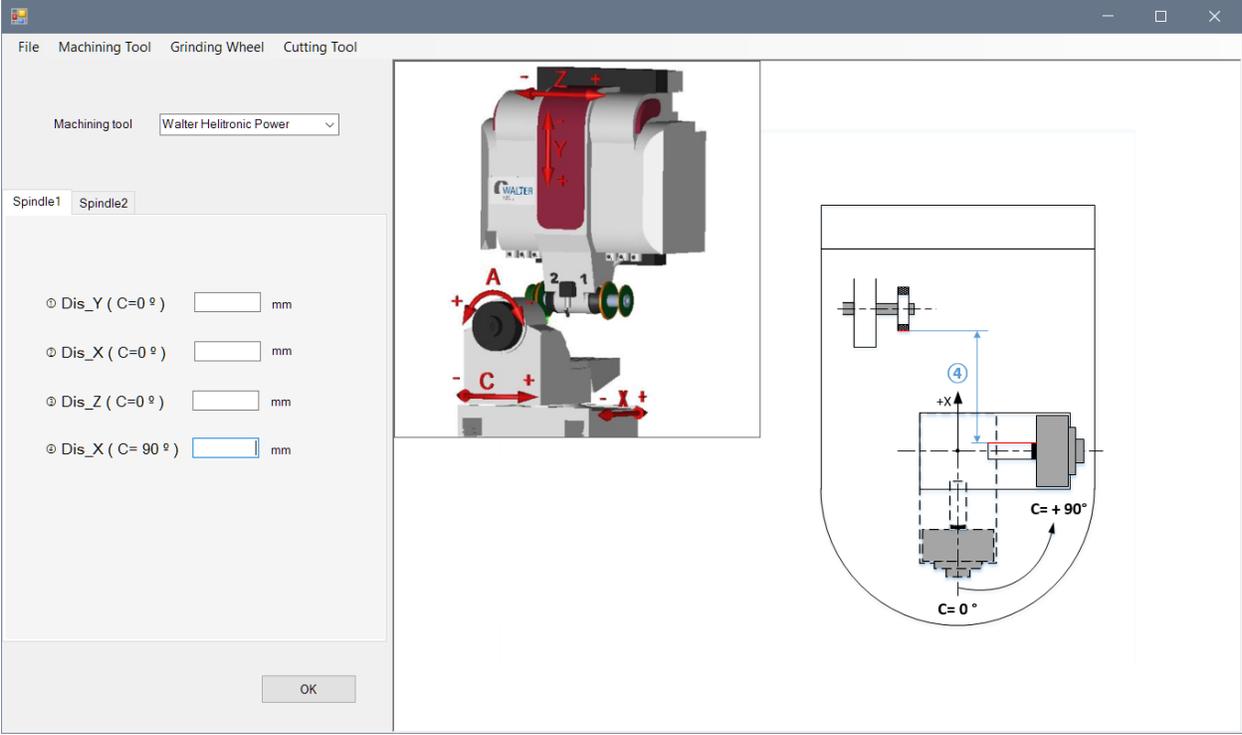
Figure 3.3 Machining tool configuration page

3.3. Grinding Wheel Workbench

For manufacturers, grinding wheels provide an efficient way to shape and finish metals and other materials. Abrasives are often the only way to create parts with precision dimensions and high-quality surface finishes. Grinding wheels come in a variety of shapes and sizes, as in Fig.3.4, it illustrates the general shape and specific parameters of 1A1,1V1 and 12V2 type of grinding wheels.

These (a), (b) configurations are peripheral grinding wheels, in which material removal is accomplished by the outside circumference of the wheel. Wheel (c) is facing grinding wheel, in

which the flat face of the wheel can remove material from the work surface. The grinding wheel

selection should be considered based on grinding strategy. Normally, there is a mounting hole on

the central of the metal frame, the size of the mounting hole should be suitable for the spindle

diameter. The abrasive part is attached on the outside of the metal frame. As the wheel wears, it

should be always measured the abrasive wall thickness to ensure accurately cutting for every

grinding process.

(a) 1A1   (b) 1V1   (c) 12V2
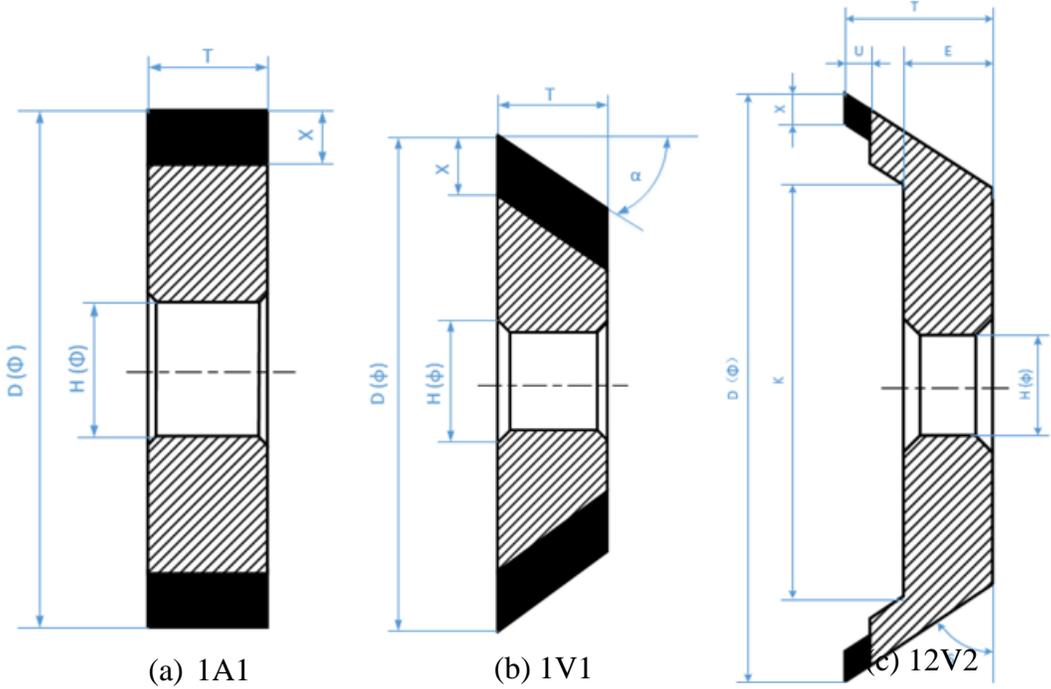
Figure 3.4 Different types of grinding wheels

The interface of the grinding wheel page can be seen in Fig.3.5.The grinding wheel workbench

allows the user to load a type of grinding wheel with specified parameters and locate at each

spindle where exactly it is. On the left side of the interface, the user can clearly know the layout

of the grinding wheel configuration for double checking whether the configured layout is the same with the layout of the CNC grinding machine.
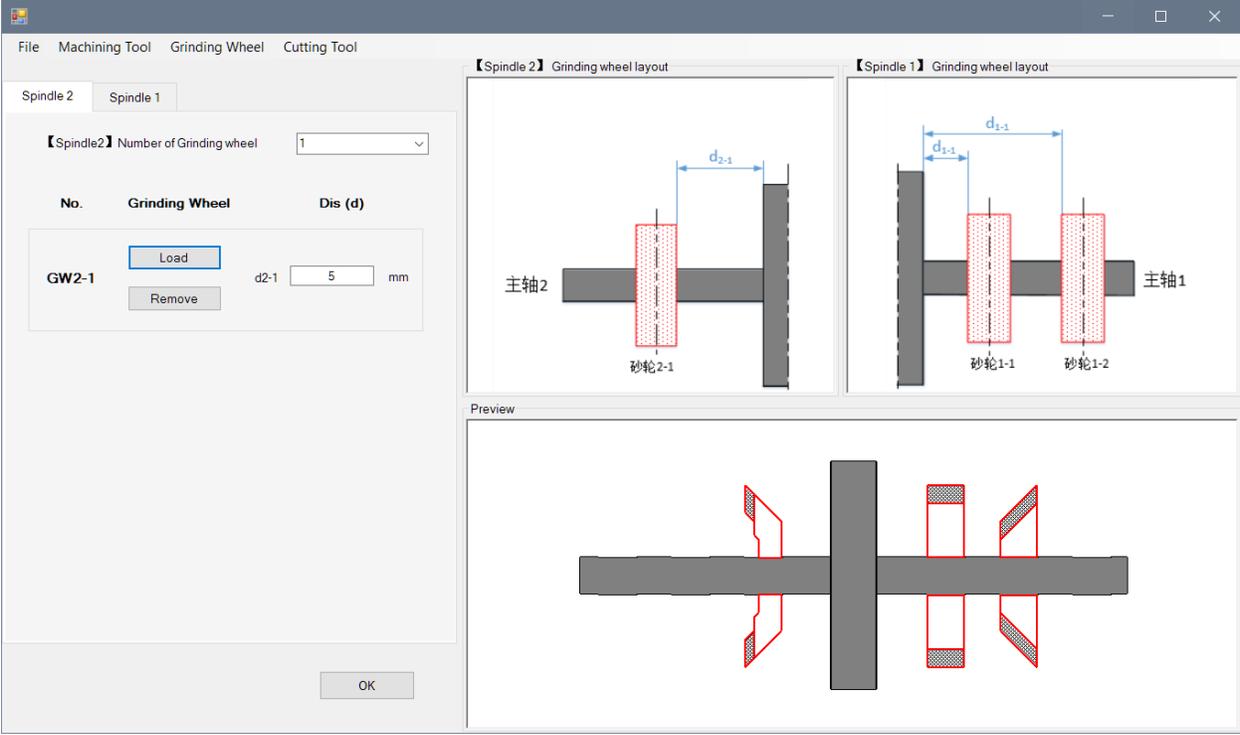
Figure 3.5 Grinding wheel page

3.4. Twist Drill Design Workbench

Twist drill design workbench consists four main features: flute, margin, point and split. The 3D model of a twist drill can be automatically built in CATIA by completely setting up every design page of each feature.

3.4.1. Flute modeling

The shape of flute has a significant influence in chip evacuation process when the drill is twisting in the workpiece. Generally, larger flute space is useful for the chip flowing, however, that will

45

decrease the tool stiffness. Therefore, it is really important to give an accurate flute model to improve the dynamic behavior and working performance.

Flute is machined by the grinding wheel moving with the helix motion with constantly adjusting position and orientation. Liming [5] proposed a kinematic model of the flute grinding process and formulate several important design parameters including tool diameter, rake angle, core diameter, flute angle, helix angle and flute length through differential geometry and coordinate transformation. Besides, he also proposed a method to calculated the position and orientation of grinding wheel instantaneously. Based on Liming's method, a 3D flute model can be generated and the grinding path of which can be obtained as well.

The user can update the information of grinding wheel in grinding wheel workbench, and load the edited grinding wheel from flute design page. It is can be seen in Fig 3.6. The rest of design parameters are available to define in the following text boxes.

Fig.3.7 shows the geometry of the flute feature. Through these defined parameters, the software will call the packaged m file to calculate flute profile and grinding path. At the very beginning, tons of discrete points will be plotted in CATIA to form the designated flute profile which is shown on the top of tool bar. The flute shape in CATIA can be generated by sweeping this flute profile in a particular helix angle and pulling down along the Z-axis.
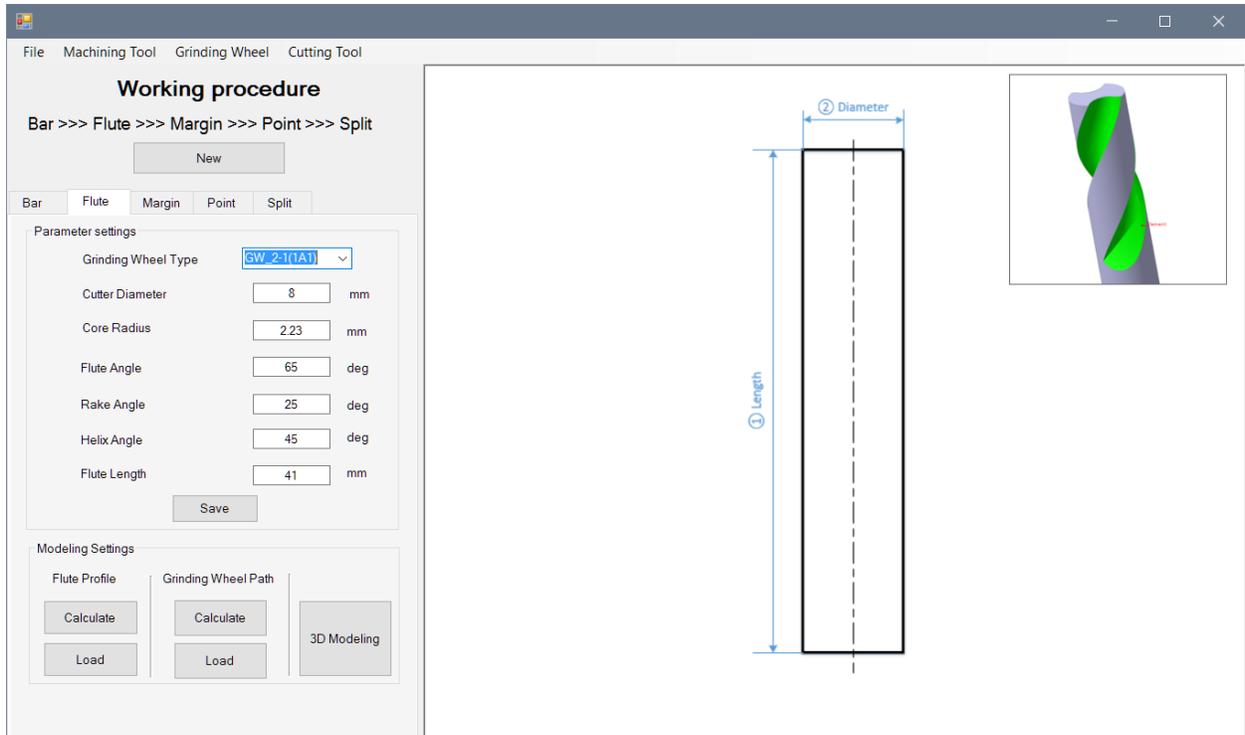
Figure 3.6 Flute design page
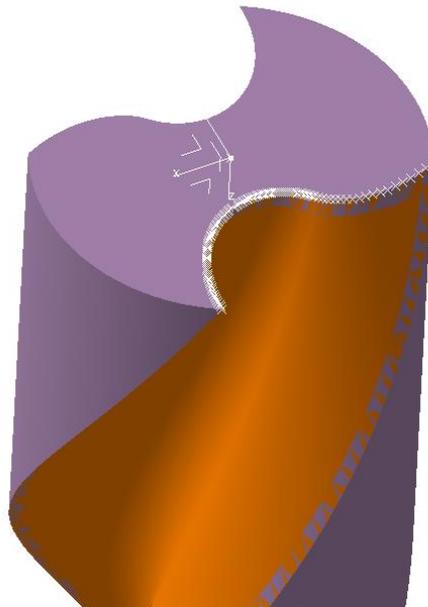
Figure 3.7 Flute modeling in CATIA

3.4.2. Margin modeling

Margin has two parts: the cylindrical portion of the land which is not cut away is constantly attached to the inside wall of the drilled hole when the twist drill is drilling into the workpiece. It provides maximum the stability to the drilling process and ensures the quality of the hole. Another part is called body clearance. This part is reduced in diameter and used for preventing excessive friction and rubbing resulted from the twisting process.

There are five crucial parameters involved in margin design: cutter diameter, core radius, clearance diameter, land width, flute length. The modeling steps are the same as the way of modelling the flute feature. The orange surface indicates the margin surface formed by sweeping margin profile along the helix line. The final margin model can be accomplished by trimming the margin surface out of the model, which is shown in Fig.3.8.
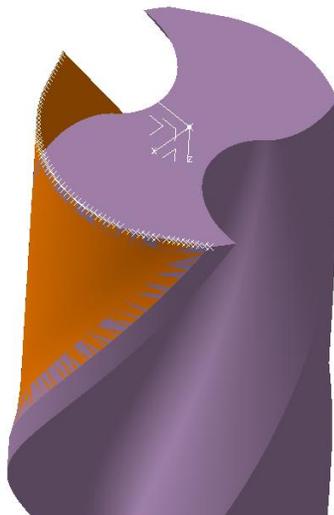
Figure 3.8 Margin modeling in CATIA

3.4.3. Point modeling

As mentioned in the previous chapter, the drill point is formed by two conical surfaces, which is shown in Fig.3.9. There are five design parameters in point design: semi point angle, chisel edge angle, lip relief angle and rest of two parameters can be specified by engineering experience. Through these five design parameters, the cone can be transformed by three translational directions and one rotary direction to the corresponding position in terms of drill axis system. The drill point model can be obtained by trimming with designed conical surfaces. The trimmed drill point model can be seen in Fig 3.10
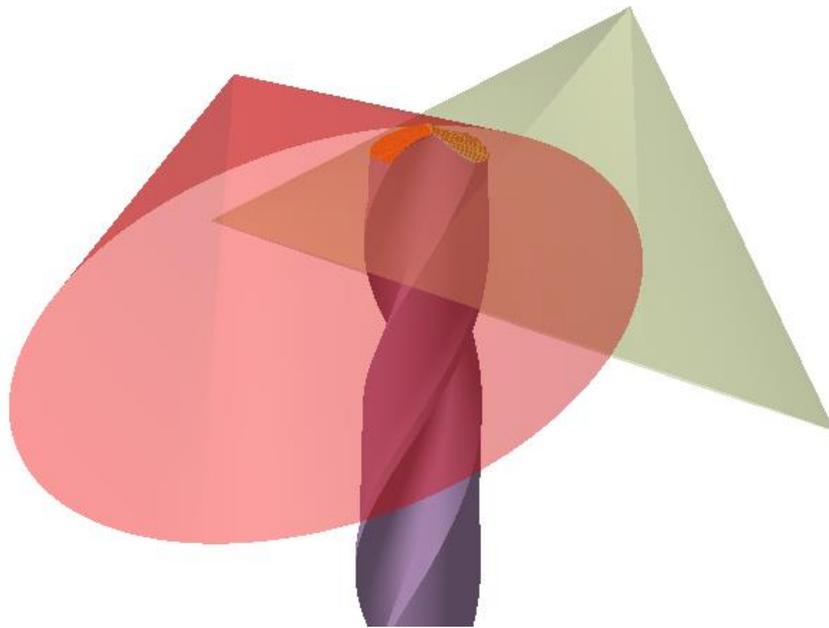
Figure 3.9 Two conical surfaces
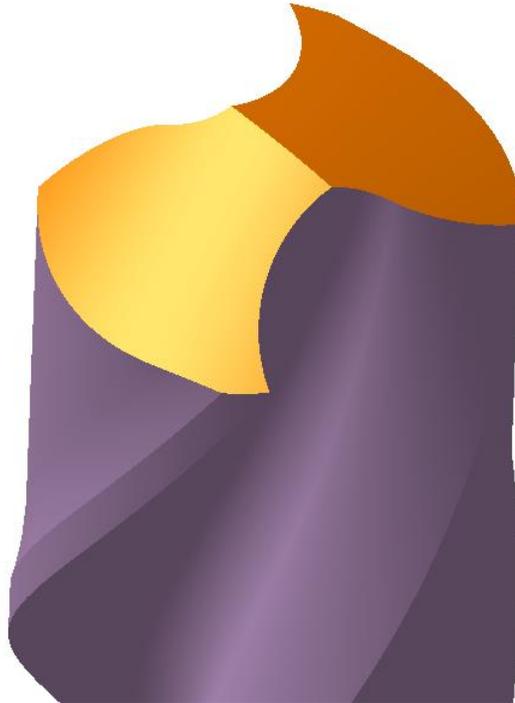
Figure 3.10 Drill point modeling in CATIA

3.4.4. Split modeling

The split profile is defined by four design parameters which is illustrated in Fig.3.11. In CATIA, we can create a sketch and easily constraint this split profile as required. And then, we can derive six points as control points, and measure the position for each of them on the xy plane. This split profile is the path that the grinding wheel will go along with.
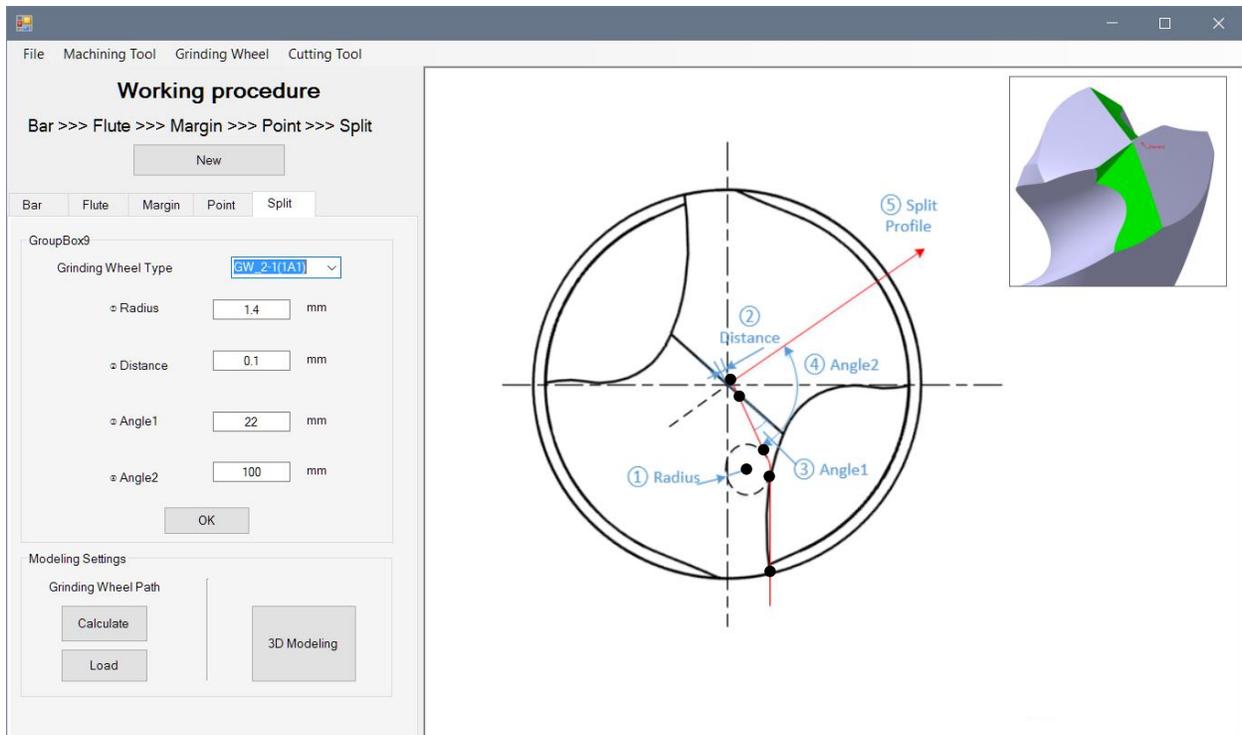
Figure 3.11 Split design page

The final split shape is made by Boolean operation. When we obtain the grinding path, it is
feasible to build many grinding wheel models at each corresponding position. See in Fig 3.12.
We remove each generated grinding wheel out of the existing model, the final split model would
be built. It can be seen in Fig. 3.13.

Figure 3.12 Position and orientation of the grinding wheel for split modeling

Figure 3.13 Split modeling in CATIA

52

Chapter 4. Application of CAD/CAM/CAE Integration of Twist Drill

Design to Predict Cutting Force

4.1. Validation of the Proposed Method of Twist Drill Design

To demonstrate the reliability of the software and all mathematic models involved for each

feature (flute, margin, point, split), four groups of design parameters of twist drill are selected for

the comparison. Corresponding 3D models of these four designs are built in CATIA through

making use of functions in the software. Besides, for each set of experimental data, it contains

two manufactured samples which are ground by Walter 5-axis grinding machine. Fig. 4.1 shows

different views of both the CATIA 3D model and the manufactured model of each experimental

data. The comparison in appearance can be clearly seen. Additionally, all the design parameters

of each manufactured twist drill are also measured and listed in Table 4-1. It shows that the

required design parameters of each experimental group have a good agreement with the

manufactured one.
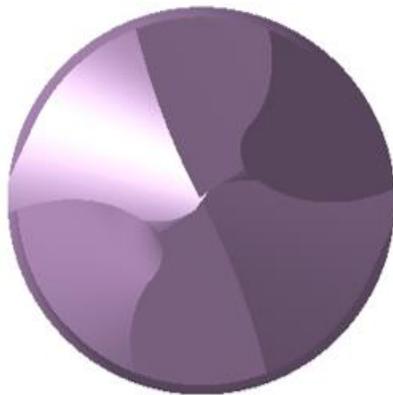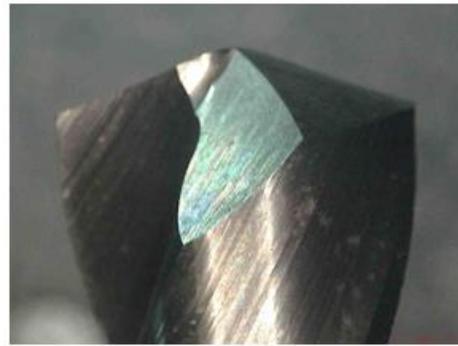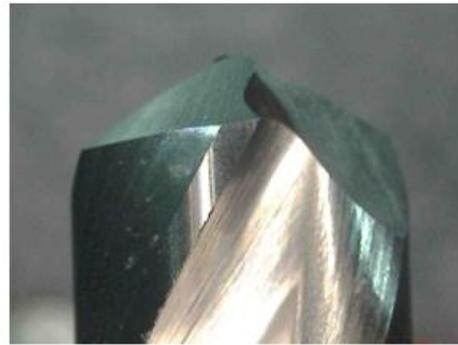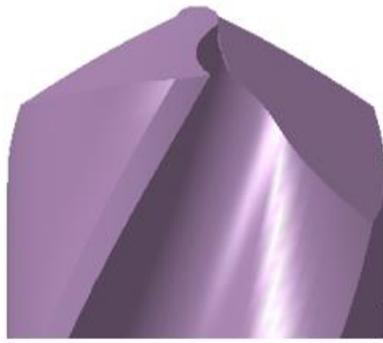
(a) Test No.1.
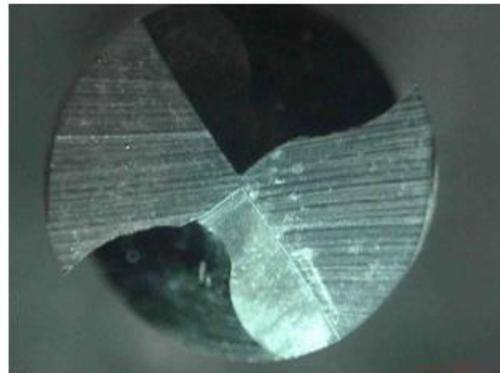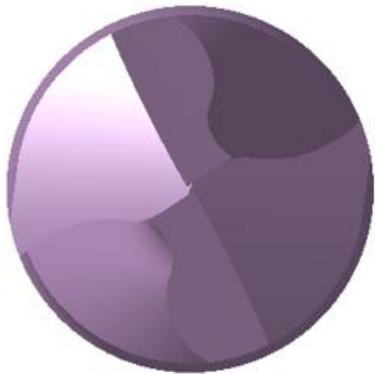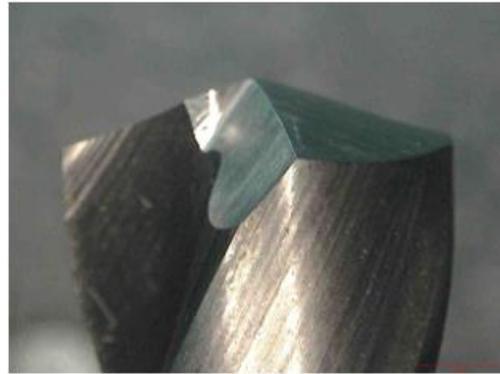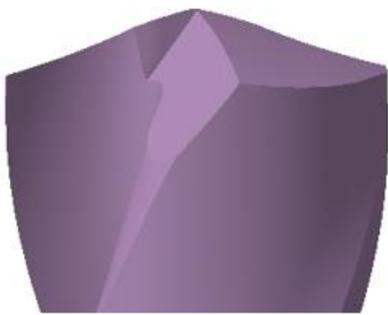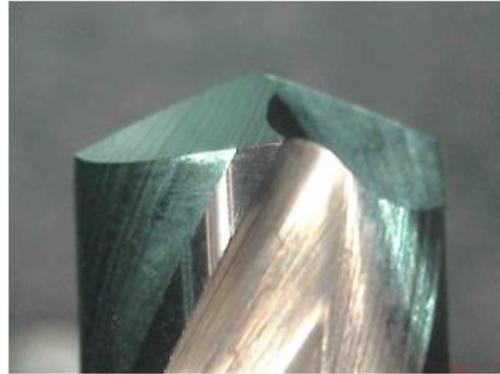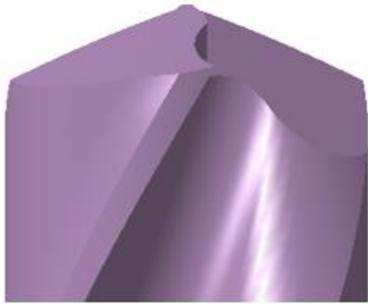
(b) Test No.2.
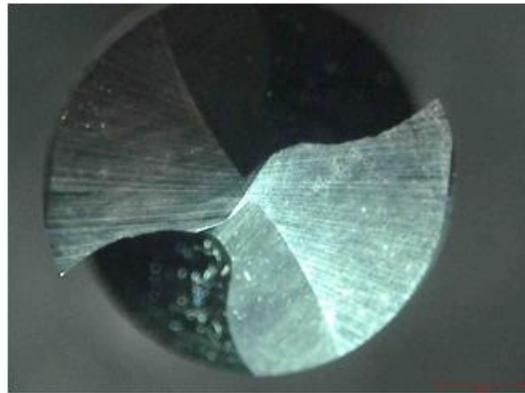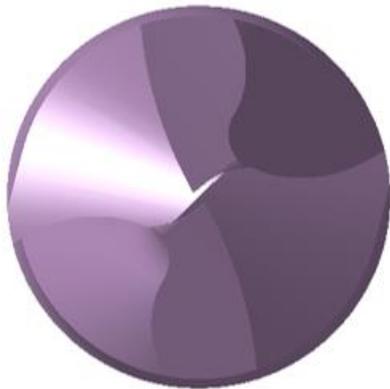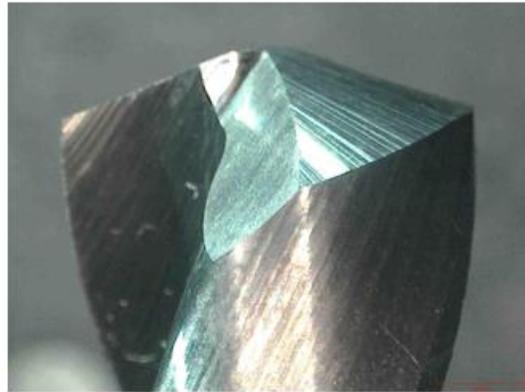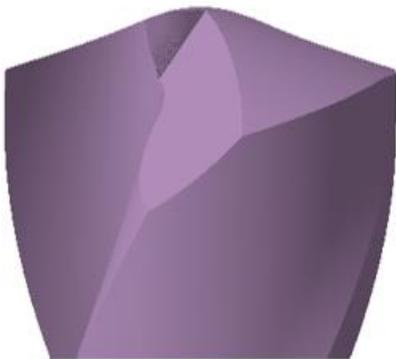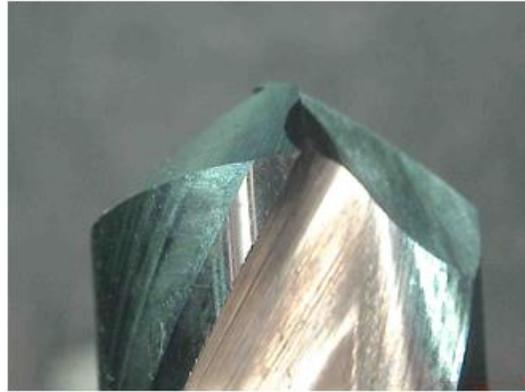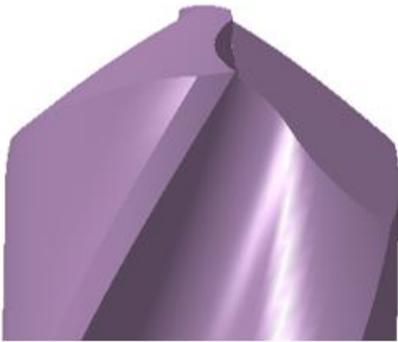
(c) Test No.3.
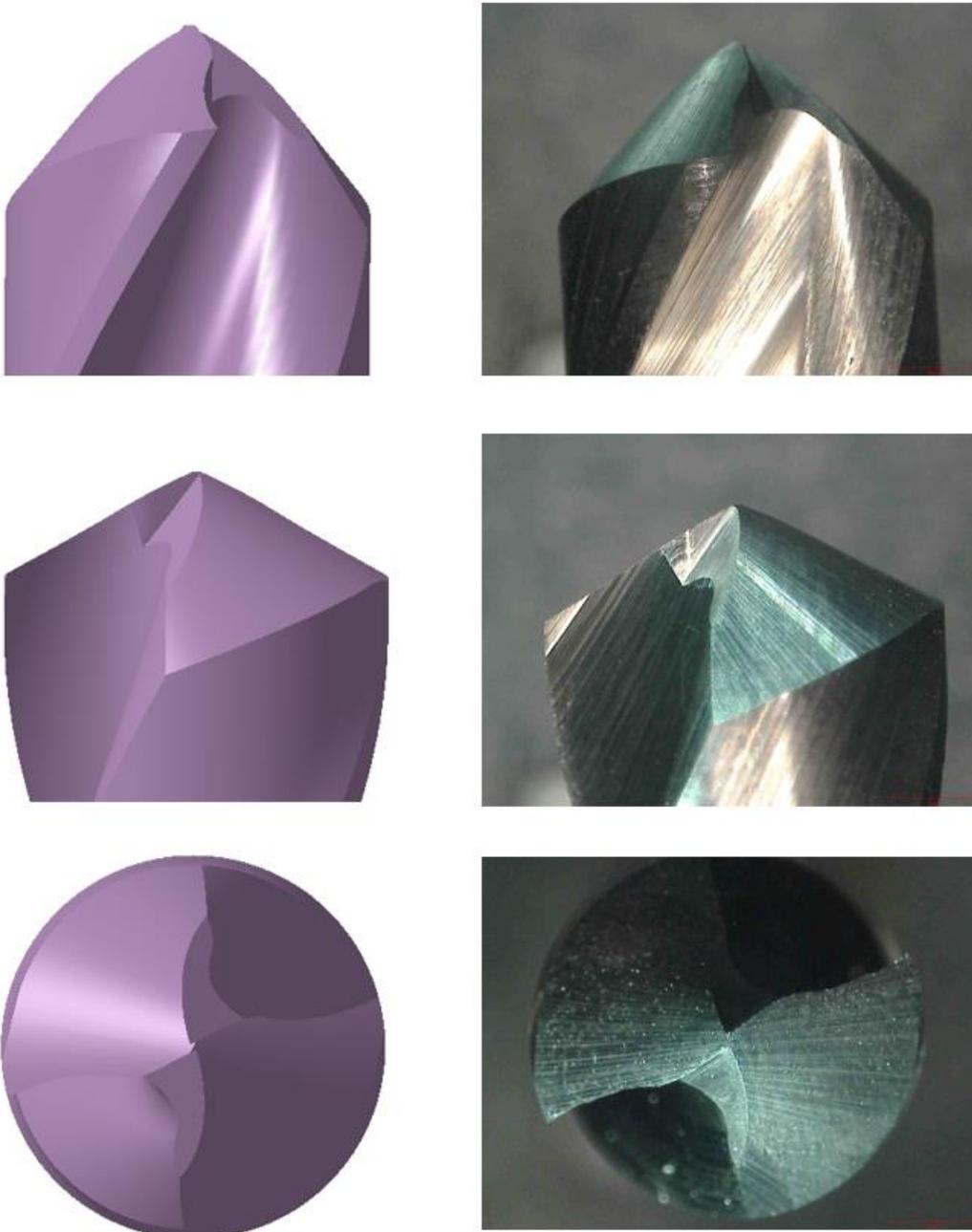
(d) Test No.4.

Figure 4.1 The comparison between CATIA model and manufactured model

Table 4-1 Designed data and measured data on manufactured drill model for each feature

Test No.	Measurement	Point			Split		
		Point angle	Chisel edge angle	Lip relief angle	Gash depth	Secondary edge offset	Secondary edge angle
1	Dimension	140°±2°	55°±3°	7°±1°	$0^{+0.05}_{0}mm$	0.08 ±0.01mm	33°±2°
	Sample 1-1	139°	57.1°	7.6°	0.01mm	0.1 mm	33.6°
	Sample 1-2	139.6°	58°	7.2°	0.01 mm	0.1 mm	32°
2	Dimension	140°±2°	55°±3°	12°±1°	$0.03^{+0.05}_{0}mm$	0.08 ±0.01mm	20°±2°
	Sample 2-1	140°	55.5°	11.5°	0.04 mm	0.1 mm	19.5°
	Sample 2-2	140°	53°	10.8°	0.035 mm	0.1 mm	19.5°
3	Dimension	140°±2°	40°±3°	7°±1°	$0.03^{+0.05}_{0}mm$	0.14 ±0.01mm	33°±2°
	Sample 3-1	140°	40°	7°	0	0.15 mm	28°
	Sample 3-2	140°	38.5°	7°	0	0.15 mm	30.5°
4	Dimension	120°±2°	55°±3°	7°±1°	$0.03^{+0.05}_{0}mm$	0.08 ±0.01mm	20°±2°
	Sample 4-1	119°	53°	7.5°	0.01 mm	0.1 mm	18°
	Sample 4-2	119°	55°	7°	0.01 mm	0.1 mm	18°

4.2. Distribution of Rake and Relief Angle Along the Secondary Cutting Edge

One of the most significant challenges to conventional drill point is the chisel edge. Chisel edge is the part of the cutting edge where the rake angle is normally negative. The negative angle along cutting edge stands for the cutting edge loses the ability to shear the material from the workpiece which results in excessive heat generation and high thrust force. Another feature of the rake angle on the cutting edge is that the angle comes gradually negative as the cutting edge going near to the center. A good way to avoid this undesirable working phenomenon is to reduce the length of chisel edge through splitting the web and creating a secondary flank surface. With the benefit of this, not only the rake angle along the cutting edge could be remained on the stable level with a positive value, but the thrust force when the drill is drilling into the workpiece are more likely to be reduced dramatically. Besides, the split feature can also positively affect the variation of relief angle along the cutting edge.

In order to compare the effect of the rake angle and relief angle of the secondary cutting edge, test drill #2 is selected as an experimental object. The first model is the conventional drill point which only contains conical flank surface on the point. For the second model, split feature is added on the conventional point structure. Both models share the same conical surface structure. Parameters of two models are listed in Table 4-1. For the cutting edge of the second model, the whole cutting edge is divided into two pieces: the primary cutting edge shares the same geometry with the first model, and the secondary cutting edge is formed by the split feature. Two models can be seen in Fig4.2.
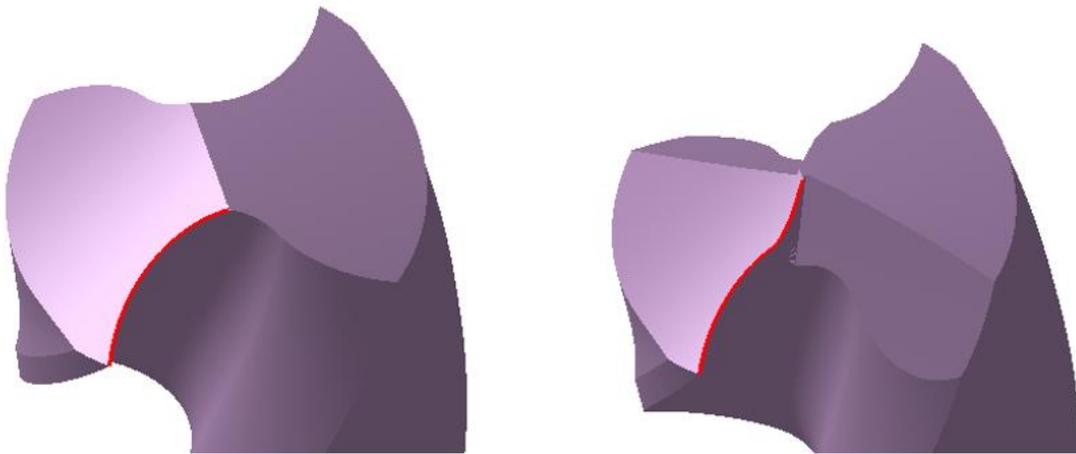
Figure 4.2 Cutting edge on the conventional point and the split point

The rake angle and relief angle along the cutting edge are measured separately on both conventional model and split model. As can be seen in Fig.4.3, the blue line with the square mark represents the variation of the rake angle measured on conventional drill point model, and the solid blue line refers to the distribution of the rake angle after splitting the conventional drill point. Similarly, the orange line shows the condition of relief angle on the cutting edge. In the conventional drill point, rake angle can be inspected a dramatic downtrend since the measurement point coming closer to the drill central point. In the split drill point, rake angle gets rid of the continuous drop starting from the intersection point of primary cutting edge and secondary cutting edge. The length of the chisel edge is measured as 0.27863mm in the split point, but this value is 2.27mm in the conventional model. Therefore, it clearly shows the split feature gives a shorter chisel edge and greater rake angle, which provides a great help to reduce the thrust and torque.

60
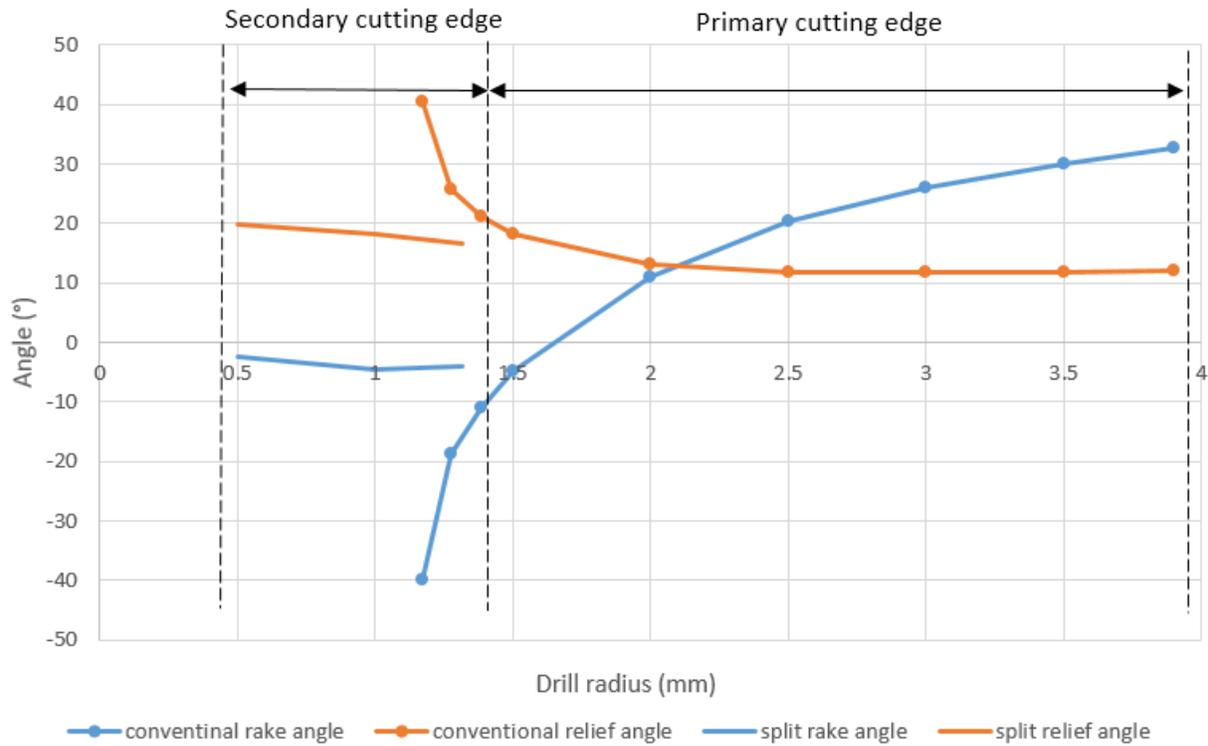
Figure 4.3 Distribution of rake angle and relief angle on secondary cutting edge

4.3. Cutting Performance Prediction

4.3.1. Introduction

The modeling method of conical twist drill is introduced in above chapters. After obtaining an accurate 3D model, finite element analysis can be used for predicting cutting force of this model. The FEA software used in this work is *Thirdwave Advantedge*, which is developed specially to estimate the cutting performance of a particular cutting tool in 2D or 3D environments based on different machining process including turning, milling, drilling, etc.

The whole drilling process can be divided into three different types: entrance, starting depth and exit. This work mainly focus on the drilling process happens on entrance and starting depth of drilling process.

4.3.2. Simulation model

In order to simulate quicker, the model of the No.2 experimental sample is trimmed and only remained 2mm height of the drill point part as the simulation model, which is shown in Fig 4.4.
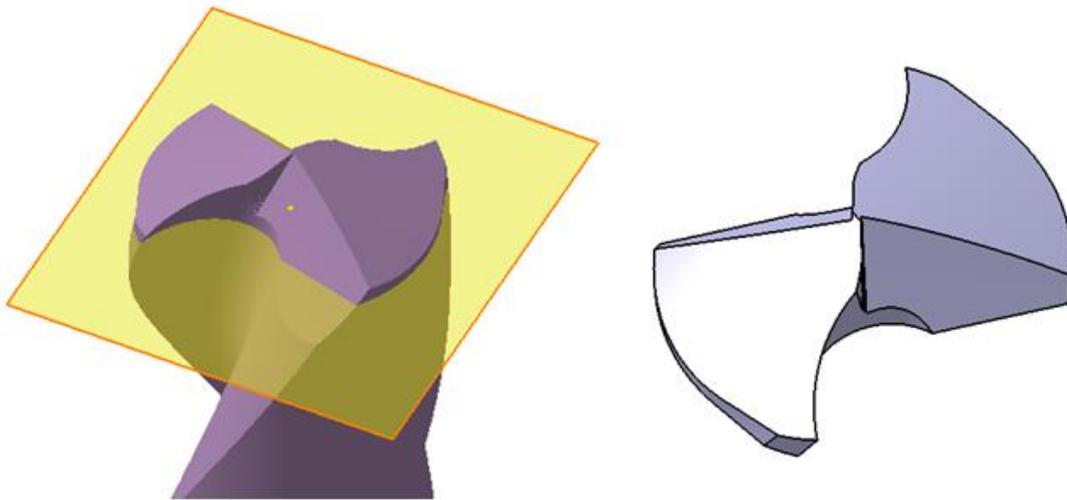
Figure 4.4 Simulation model

Design parameters of the 3D simulation model can be seen in Table 4-2. Fig. 4.5 show that the point height measured on experimental sample #2 is 1.29mm. The workpiece is a block with 10mm length and 3mm height.
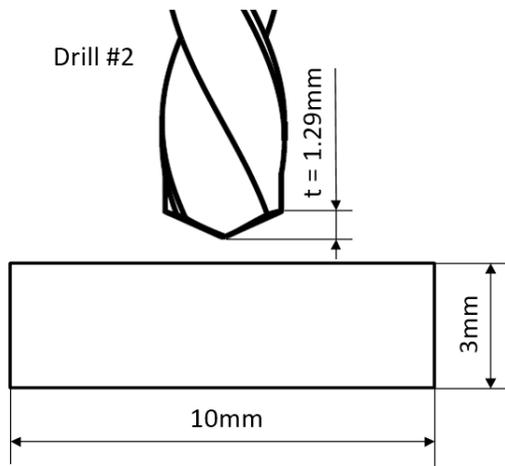
Figure 4.5 Dimensions of drill model and workpiece model

Table 4-2 Parameters of designed model and 3D simulation model

Drill parameters	Designed model	3D simulation model
Tool length	79mm	2mm
Tool diameter	8mm	8mm
Point angle	140°	140.026°
Chisel edge angle	55°	55.004°
Lip relief angle	12°	11.988°
Gash depth	0.03 mm	0.029mm
Secondary edge offset	0.08mm	0.080mm
Secondary edge angle	20°	20°

4.3.3. Material selection of tool and workpiece

D3 tool steel is used in tooling applications requiring a high degree of accuracy in hardening. Because of the abrasion resistant nature, machining in the hardened condition should be limited to finish grinding. Cemented carbide is the material with a great hardness and widely used in cutting tool for machining. The most advantage of this material is cemented carbide has a very good abrasive resistance performance and can also resist higher temperature rather than standard high-speed steel. And the cemented carbide cutting tool normally maintains a sharp cutting edge better than other materials, they are able to produce a better fishing on the workpiece. *Thirdwave* material database provides the material properties of D3 tool steel but cemented carbide material properties are not offered in *Thirdwave* so it should be customized by the user. Table 4-3 lists all properties of the material needed for both cutting tool and workpiece in this simulation.

Table 4-3 Material properties of twist drill and experimental workpiece

Properties	Twist drill	Workpiece
material	Cemented carbide	D3 tool steel
Density	14800 kg/ m³	-
Heat capacity	39.8 J/mol·K	-
Thermal conductivity	110 W/(m·K)	-
Poisson's Ratio	0.31	-
Young's Modulus	530-700 Gpa	-

4.3.4. Process parameters

According to the workbook [16] published by Edward G. Hoffman. The feedratefor drilling is governed primarily by the size of the drill and by the material to be drilled. For ordinary twist drill, the feedrateused is 0.004 to 0.01 inch/rev. for the drill with the diameter of 0.25 inch to 0.5 inches. The another principle to set up the feed rate is the lower values in the feed range should be used for hard material such as tool steel, super alloys. The material in this experiment is D3 cold tool steel, the diameter of the sample is 8mm. Thus, the feedrateis selected as 0.004 in./rev, which is 0.1 mm/rev. Process parameters can be seen in Table 4-4.

Table 4-4 Drilling process parameters

Spindle speed (Rev./min.)	Feed rate (mm / rev.)	Initial temperature (°C)	Drilling depth (mm)	Cutting environment
291.2	0.1	20	1	dry

The speed of a drill to machine D3 cold-work tool steel is recommended as 30 feet/min. by Edward G. Hoffman [16]. Fig.4.6 is the drilling process demonstration in *Thirdwave* which shows that the speed is defined in terms of the rate where the outside of the cutting tool. To deliver this parameter to *Thirdwave*, this value should be converted into rpm. The relationship between fpm and rpm is

$$rpm = 3.8 \times \frac{fpm}{Drill \quad Diameter \quad in \quad Inches} \tag{43}$$
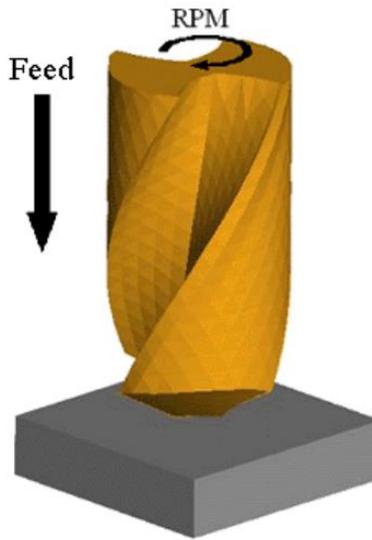
Figure 4.6 Drilling process

4.3.5. Simulation result

As mentioned above, this simulation work focuses on entrance process and starting depth process. At the very beginning of drilling process, chisel edge is the first part to touch on the workpiece. With the drill point drilling into the material, cutting force, torque and temperature will reflect different variation. Thrust is the cutting force along z-axis. This simulation work will analyze the drilling performance mainly referred from thrust, torque, and temperature.

Because of point height of experimental sample #2 is 1.29mm, the simulation motion of the entrance process is set from the original position to getting down by 1mm. In order to simulate the process that drill point completely drilling into a workpiece during starting depth process, the simulation will start from 1.8mm depth and go 0.2mm deep. The simulation configurated of two processes is demonstrated in Fig.4.7.

66
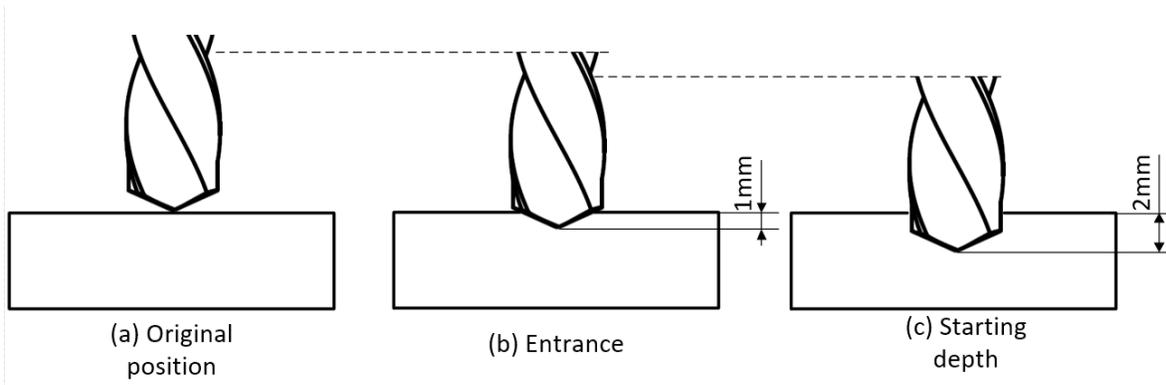
Figure 4.7 Drilling simulation process: entrance and starting depth.

Fig. 4.8 show meshing status of the workpiece and 3D simulation model at the original position. The general dimension and configuration can be clearly seen as well. The mesh size along cutting edge of the 3D simulation model is defined as 0.05mm.
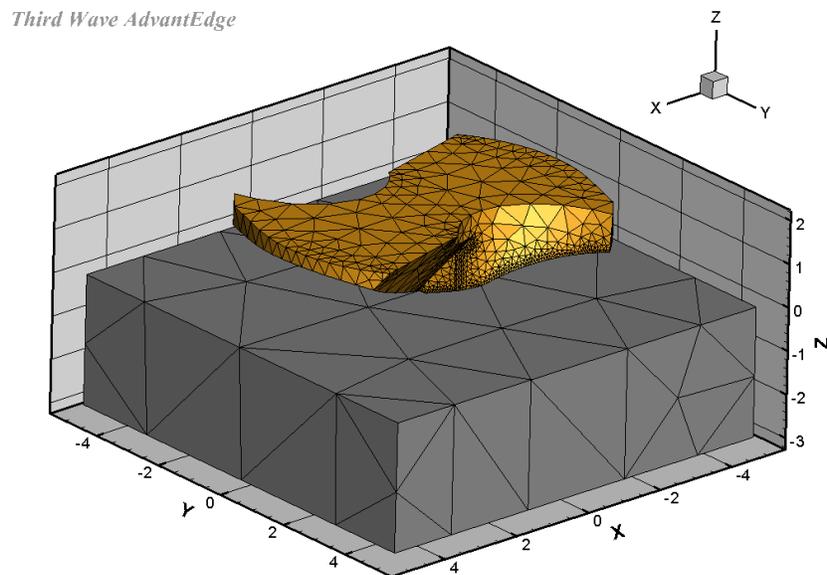
Figure 4.8 Meshing of the 3D simulation model

Fig.4.9 illustrates that the simulation result of entrance process, where can be found that cutting

force mainly results from the thrust force. When the drill tip touches the workpiece, thrust force

increases dramatically. It is because chisel edge starts to attach to the material, and the negative

rake angle on chisel edge acts huge thrust on the axial force. Then, with the cutting edge

gradually working on the workpiece, the cutting force raises correspondingly and torque goes up

as well. Temperature is highly related to the linear velocity of the point on the cutting edge, the

outer area it goes, a higher temperature will be produced. Fig.4.10 shows the cutting performance

prediction simulated by *Thridwave*.
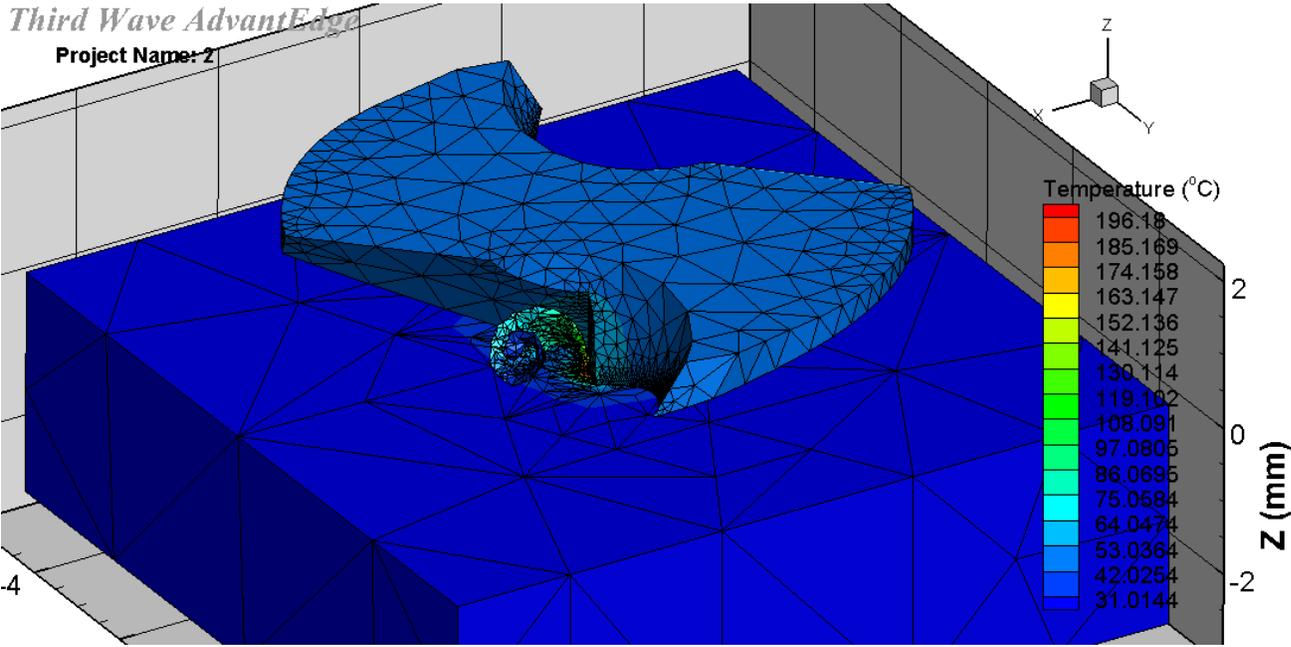
Figure 4.9 Drilling simulation of entrance process in *Thirdwave*
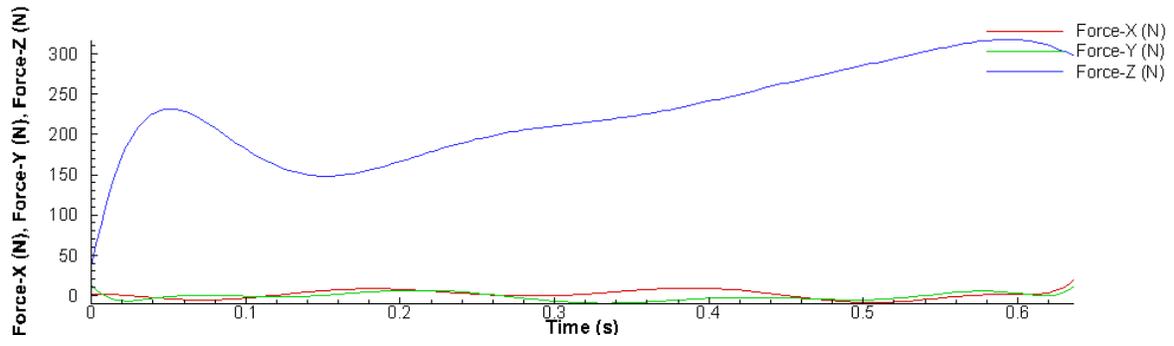
(a) Cutting force
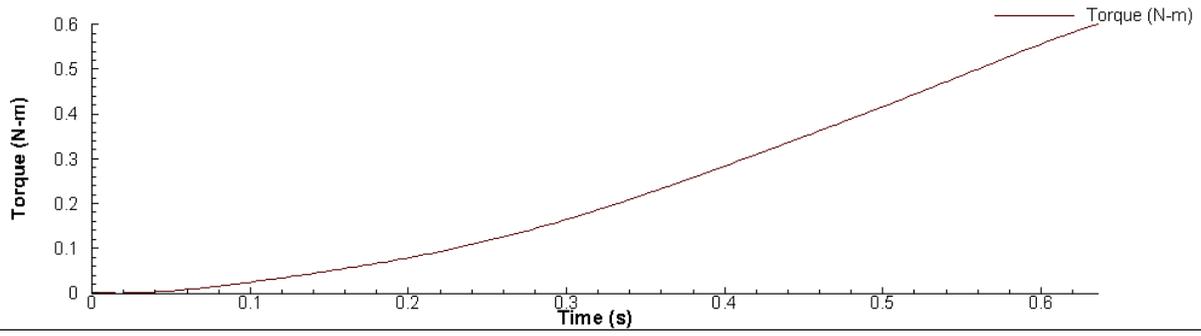
(b) Torque
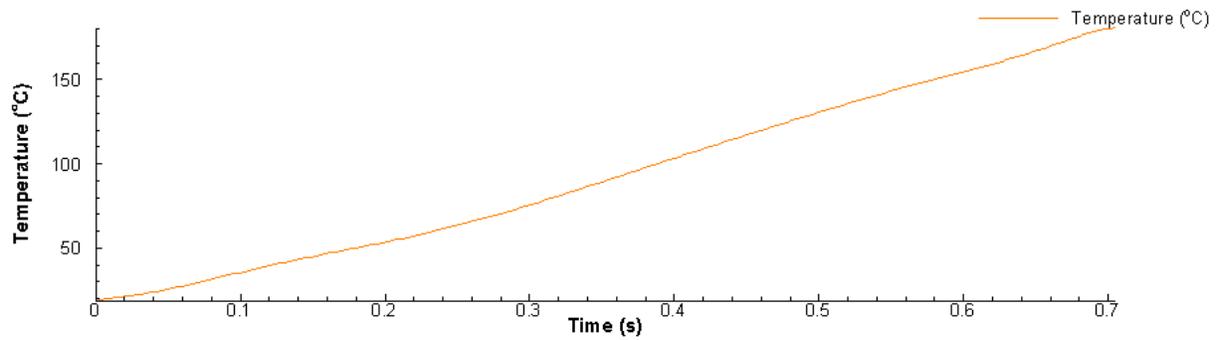
(c)Temperature

Figure 4.10 Prediction result of entrance process in *Thirdwave*

Fig.4.11shows the starting depth process that drill point completely plunges into the workpiece and entire cutting edge is shearing chips out of the workpiece. The hole generated in this drilling process is shown in Fig.4.12. It is clearly noticed an obvious mark is left on the bottom surface of the hole. It is because when the simulating time is up, *Thirdwave* will suddenly stop to calculate. This phenomenon is not like the reality which the spindle is supposed to stay at the ending position with the same spindle speed and afterward pull up the drill. In this period, the bottom surface will be finished better. As we can see in Fig.4.13, the temperature goes gradually up with the distance increasing along the cutting edge from center to outer corner.
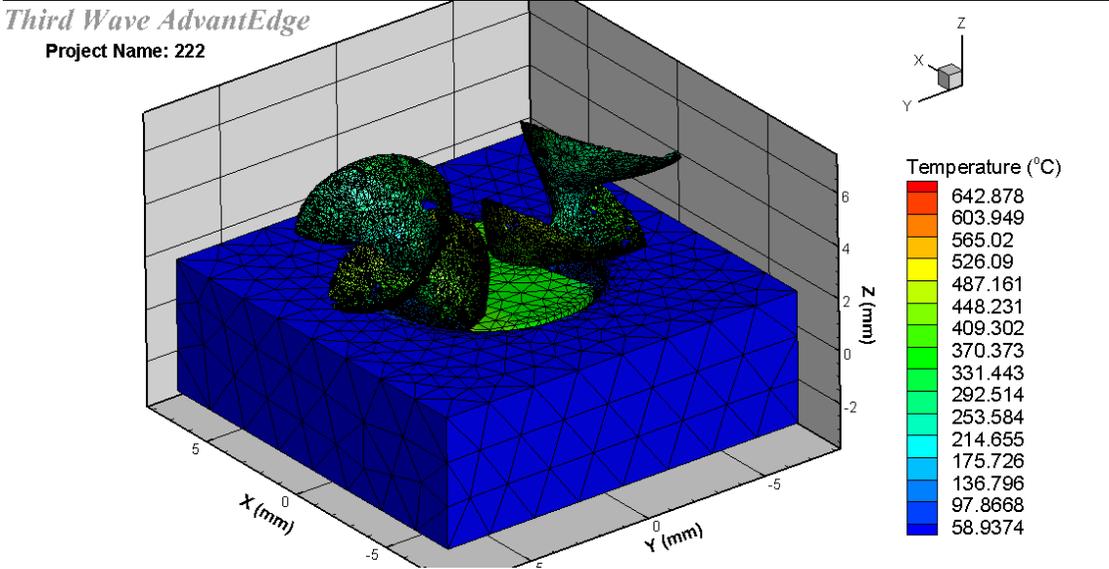
Figure 4.11 Drilling simulation of starting depth process in *Thirdwave*
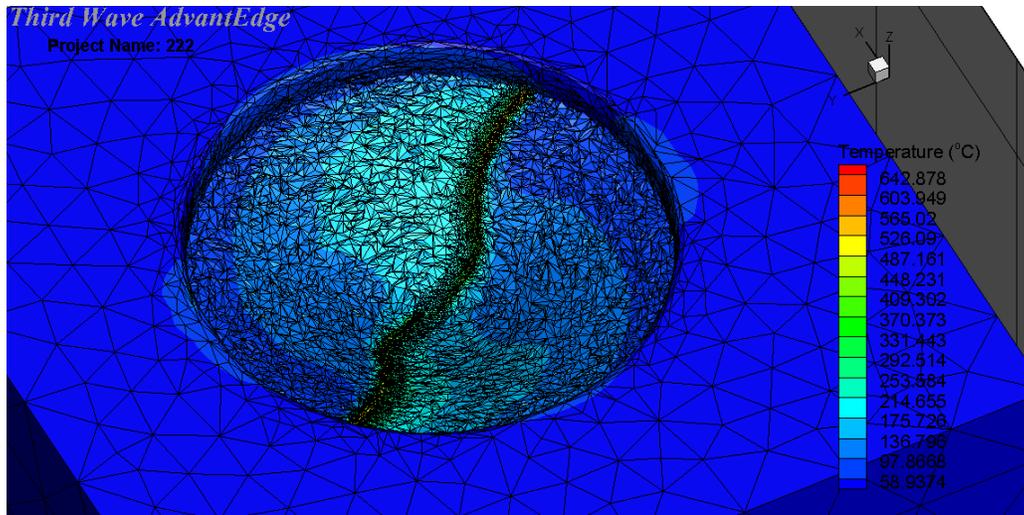
Figure 4.12 Generated hole in *Thirdwave*
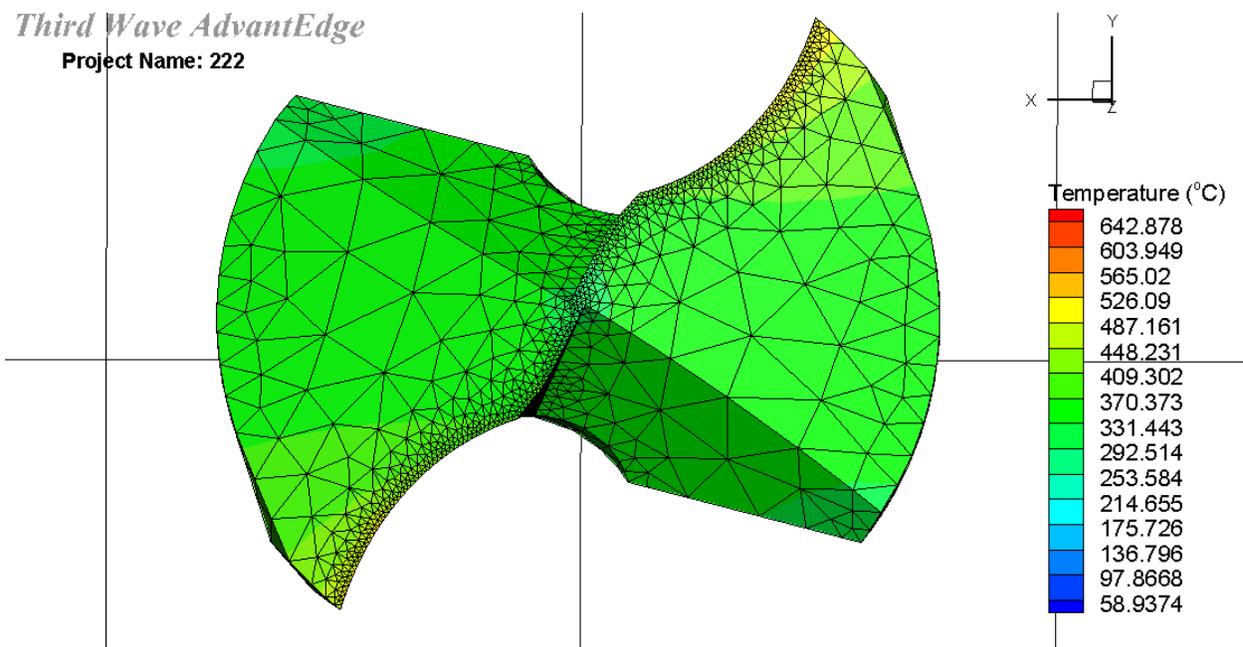
Figure 4.13 Temperature distribution along cutting edge

In this process, cutting edge entirely takes a great effect on the workpiece which makes thrust

reach to a relatively stable phase. The maximum of the thrust is 500N. Figure 4.12show the

generated hole in this simulation. The torque shows a big jump up to 7 N·m at the first beginning when the spindle rotates by 50 degrees, then drops down to 5.2 N·m and remains around 5.4N·m. Temperature goes slightly up because of the friction generated by cutting when the high-rotating drill point plunging in the material.
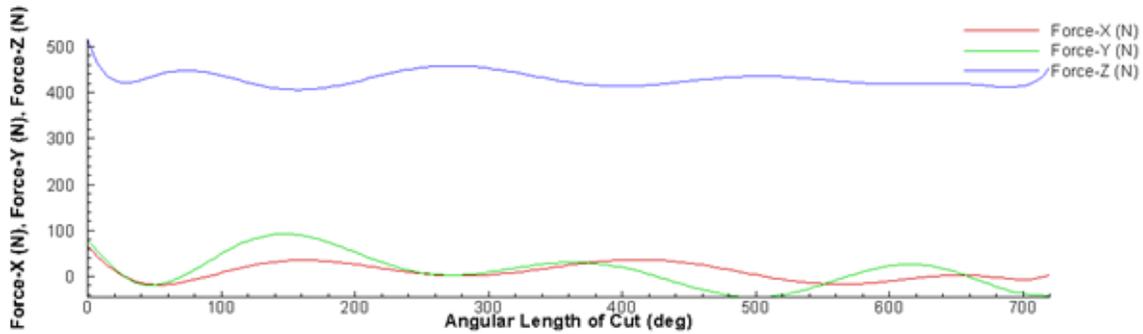
(a) Cutting force
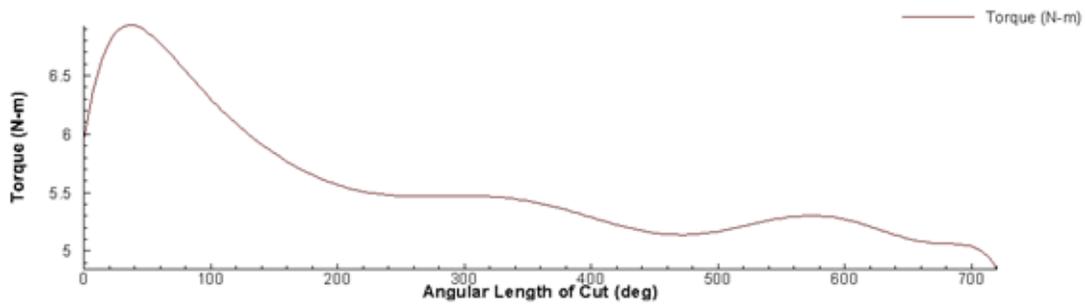
(b) Torque
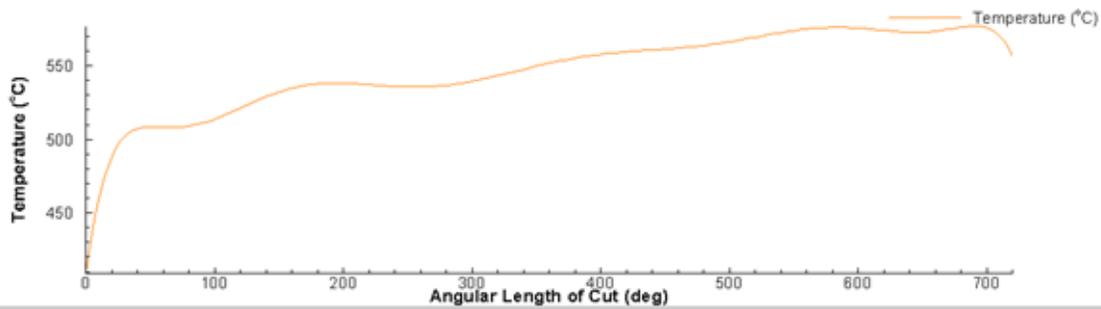
(c) Peak temperature

Figure 4.14 Prediction result of starting depth process in *Thirdwave*

Kožmín and his colleagues [17] in 2010 made experiments to predict the cutting force by using cemented carbide drill to cut D3 cold work mold steel. In his experiment, the thrust and torque are as much as 2600N and 11N·m, respectively. It means that the cutting tool made of cemented carbide can at least bear up to 2600N of thrust and 11N of torque. In my simulation work, the maximum thrust = 500N, torque = 7N·m and the peak temperature is 550 °C. These data are all qualified with the reference given by Kožmín's experiment. Therefore, the cutting performance of this designed drill is acceptable.

Table 4-5 Comparison between the simulation and Kožmín's experiment

	Maximum thrust (N)	Maximum torque (N·m)	Maximum peak temperature (°C)
My simulation	500	7	550
Kožmín's experiment	2600	11	850

Chapter 5.   Conclusion and Future Work

5.1. Conclusion

In this project, all the work is related to the new approach to design the conical twist drill point. Based on the derived mathematic model, an automatic modeling software is developed and the improvement on working performance of the split point with regard to the conventional drill point is analyzed. The major work can be concluded as follows:

1) The mathematic model of conical drill point is established. Based on this mathematic model, grinding parameters can be directly solved by a group of given design parameters. After that, 3D model of this designed conical drill point can be built in CATIA which is feasible to check out the structure and quickly modify the design. The effect of grinding parameters on each design parameters is presented. The mathematic model is verified by comparing the required design parameters and the parameters measured on the model, the result indicates the proposed conical point model is accurate and workable.

2) An integrated CAD/CAM software is developed. This software integrates CATIA automation technique and the manufacturing calculation of a twist drill. It provides a user-friendly interface to users. Even the one without a strong design background can easily use it and accomplish the design work. By following several easy steps, a 3D model will build in CATIA automatically and grinding path will be outputted as well.

3) A group of designed experimental samples is manufactured by Walter 5-axis grinding machine. Design parameters are measured on these manufactured samples and compared

with required ones. The difference between these two set of data is really small and acceptable. It verifies the reliability of the proposed model. Furthermore, the distribution of rake angle and relief angle is analyzed along the split cutting edge and the conventional cutting edge separately and found that the existence of the split feature avoids rake angle dropping sharply when the cutting edge comes close to the center. The cutting force is predicted in *Thirdwave Advantedge* software. It also shows that the cutting performance of this designed drill is acceptable.

5.2. Future Work

For the future work, the following directions can be suggested to expand the current work:

1) The machining process simulation can be added in the integrated CAD/CAM software. Currently, the grinding path exported from the software is only according to the basic calculated position and orientation of grinding wheel. The present way to verify this grinding path is by converting it into G-code and directly deliver to CNC machine to test in a real grinding experiment. However, any machine operation, the usage of material and potential machine crash could result in an unimaginable cost and the delay for your manufacturing schedule. *Vericut* is a commercial software can accurately simulate grinding path motion, material removal, detecting potential error may happen in the machining process. With the help of *Vericut*, the designer is able to maximum save the cost of experiment and reduce the risk taking.

2) 3D models can be optimized with the use of cutting performance prediction method in *Thirdwave*. More models can be built in the integrated CAD/CAM software, relationships

between relative design parameters and cutting performance afterward could be investigated. It helps to provide a reference to search a optimized structure of the twist drill in terms of a particular material.

References

[1] Amirouche, Farid ML. *Principles of computer-aided design and manufacturing.* Pearson/Prentice Hall, 2004.

[2] Dieter Ziethen, *CATIA V5: Macro Programming with Visual Basic Script.* Mcgraw-Hill, 2013

[3] Groover, Mikell P. *Fundamentals of modern manufacturing: materials processes, and systems.* John Wiley & Sons, 2007.

[4] D.F. Galloway, "Some Experiments on the Influence of Various Factors on Drill Performance", Transactions of the ASME, 1957, pp. 191–231.

[5] S. Fujii, M. F. Devries and S. M. Wu, "An analysis of drill geometry for optimum drill design by computer, Parts I and II, Drill geometry analysis; Computer-aided design", Journal of Engineering for Industry, Transactions ASME, Series B, 92, pp. 647–666, 1970.

[6] Tsai, W. D., and S. M. Wu. "A mathematical model for drill point design and grinding." *Journal of Engineering for Industry* 101.3 (1979): 333-340.

[7] Radhakrishnan, T., S. M. Wu, and C. Lin. "A mathematical model for split point drill flanks." *Journal of Engineering for Industry* 105.3 (1983): 137-142.

[8] Fugelso, M. A. "Conical flank twist drill points." *International Journal of Machine Tools and Manufacture* 30.2 (1990): 291-295.

[9] Ren, Kaichun, and Jun Ni. "Analyses of drill flute and cutting angles." *The International Journal of Advanced Manufacturing Technology* 15.8 (1999): 546-553.

[10]   Paul, Anish, S. G. Kapoor, and R. E. Devor. "A chisel edge model for arbitrary drill point geometry." *Journal of Manufacturing Science and Engineering* 127.1 (2005): 23-32.

[11]   Zhang, Wei, Fengbao He, and Dilin Xiong. "Parameterized geometric design for complex helical drill point." *Journal of manufacturing science and engineering* 127.2 (2005): 319-327.

[12]   Vijayaraghavan, Athulan, and David A. Dornfeld. "Automated drill modeling for drilling process simulation." *Journal of Computing and Information Science in Engineering* 7.3 (2007): 276-282.

[13]   Li, M. Y., Tao Shen, and D. Q. Wang. "The Simulation Measurement of Standard Twist Drill's Angle Based on PRO/E." *Modular Machine Tool & Automatic Manufacturing techniques* 3 (2010): 68-70.

[14]   Lin, Psang Dain. "Computer Numerical Control Grinding Wheel Pose for Thinned/Notched Drill Points with Specifiable Secondary Cutting Edge and Characteristic Angles." *Journal of Manufacturing Science and Engineering*136.4 (2014): 041002.

[15]   L.M. Wang, and Z. Chen. "A new CAD/CAM/CAE integration approach to predicting tool deflection of end mills." *The International Journal of Advanced Manufacturing Technology,* vol. 72, no.9-12, pp.1677-1686, 2014.

[16]   Hoffman, Edward G., Christopher J. McCauley, and Muhammed Iqbal

Hussain. *Shop reference for students and apprentices*. Industrial Press Inc., 2000.

[17]   Kožmín, Pavel, Josef Sklednička, and Pavel Roud. "FEM method in chip shape

and cutting force prediction when drilling difficult to cut materials.",2010